8 Limit Cycles, Oscillations, and Excitable Systems

One ring to rule them all, one ring to find them,
One ring to bring them all, and in the darkness bind them
J.R.R. Tolkien (1954) *The Lord of the Rings*, Part 1 Ballantine Books, NY (1965)

Periodicity is an inherent phenomenon in living things. From the cell cycle, which governs the rate and timing of *mitosis* (cell division), to the *diurnal* (circadian) cycle that results in sleep-wake patterns, to the ebb and flow of populations in their natural environment—life proceeds in a rhythmic and periodic style. The stability of these periodic phenomena, the fact that they are not easily disrupted or changed by a noisy and random environment, leads us to believe that the pattern is a ubiquitous part of the process of growth, of biochemical and metabolic control systems, and of population fluctuations.

Oscillations are easily found in such physical examples as spring-mass systems and electrical circuits, which ideally are linear in behavior. Nonlinear equations such as the Lotka-Volterra predation model yield oscillations too. However, as previously suggested, the Lotka-Volterra equations are not sufficiently descriptive of the oscillations encountered in natural population cycles. For one thing, the Lotka-Volterra cycles are neutrally stable. This means that the amplitude of oscillations depends on the initial population level. (We shall see in Section 8.8 that all *conservative systems* share this property.) Another unrealistic feature is that the Lotka-Volterra model is structurally unstable: very slight modifications of the equations will disrupt the cycling behavior (see comments in Chapter 6).

For this combination of reasons, we are led to consider more suitable descriptions of the stable biological cycles. It transpires that the notion of a limit cycle

answers this need. In phase-plane plots a *limit cycle* is any simple oriented closed curve trajectory that does not contain singular points (points we have been calling steady states and at which the phase flow is stagnant). The curve must be *closed* so that a point moving along the cycle will return to its starting position at fixed time intervals and thus execute periodic motion. It must be *simple* (cannot cross itself) by the uniqueness property of differential equations [see Figure 8.1(*a*,*b*) and problem 1].

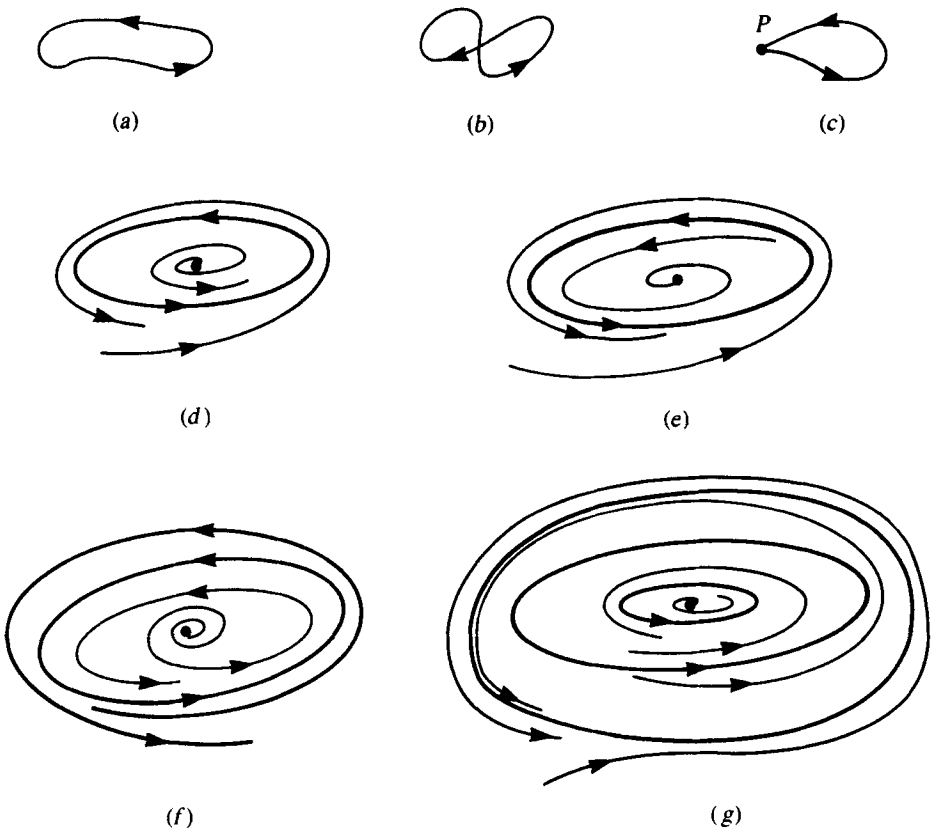

Figure 8.1 *(a) A simple closed, oriented curve. (b) This curve is not simple since it crosses itself. (c) If* P *is a steady state, this curve cannot be a limit cycle. Limit cycles come in several varieties. (d) This limit cycle is stable since all neighboring points are contained in trajectories that approach it as* $t \to +\infty$. *(e,f) These are unstable. (g) A multiplicity of limit cycles, some stable and some not, are shown.*

What distinguishes a limit cycle from the cycles that surround a neutral center (see Chapter 5) is the fact that it represents the limiting behavior of adjacent trajectories; points nearby will approach the limit cycle either for $t \to +\infty$ or for $t \to -\infty$. If the former case holds (for all adjacent trajectories) the limit cycle is *stable*. Other-

wise it is *unstable*. Figure 8.1 provides several examples of stable and unstable limit cycles in a two-dimensional phase plane.

In this chapter we are concerned with identifying criteria that point to the existence (or nonexistence) of limit cycles. We shall address this issue primarily within the context of the system of the two equations

$$\frac{dx}{dt} = F(x, y), \tag{1a}$$

$$\frac{dy}{dt} = G(x, y). \tag{1b}$$

About F and G we shall assume that these are continuous functions with continuous partial derivatives with respect to x and y so that a unique solution to (1a,b) will exist for a given set of initial values (x_0, y_0).

Before launching into the mathematical techniques that are useful in determining whether limit cycles to a system such as equations (1a,b) exist, we discuss neural excitation by way of a motivating example. Some of the basic concepts and physiological detail are described in Section 8.1. A model due to Hodgkin and Huxley is then derived and partially analyzed in Section 8.2, to be followed later by a simpler set of equations due to Fitzhugh and Nagumo in Section 8.5. We find that both models have the potential for exhibiting sustained oscillations typical of a limit cycle solution, as well as *excitable behavior:* by this we mean that a stimulus larger than some threshold will provoke a very large response. (This type of behavior is depicted by a large excursion away from some steady state and then back to it as excitation subsides.) While phase-plane analysis (described in Chapter 5) suffices for understanding Sections 8.1 and 8.2, we find it useful to draw on new results in Section 8.5.

The Poincaré-Bendixson theory is a cornerstone on which much of the theory of limit cycles rests. Section 8.3 provides an informal introduction, and the results are then applied in Section 8.4 to a system of equations known as the van der Pol oscillator. This prototype serves to illustrate how a nullcline configuration in which one or both nullclines is S-shaped tends to produce oscillatory or excitable behavior. Many examples drawn from the literature are based on similar principles. Among these is Fitzhugh's model for neural excitation described in Section 8.5.

Another mathematical method commonly encountered in the quest for limit-cycle solutions is the Hopf bifurcation theorem (Section 8.6). Here we are more specific about the spectrum of possible effects that are encountered close to a steady state of a nonlinear system at which linear stability calculations predict a transition from a stable focus through a neutral center to an unstable focus as some parameter is varied. (The comments at the end of Section 5.9 were deliberately vague in anticipation of the upcoming discussion.)

In Sections 8.7 and 8.8 we apply the new mathematical techniques to problems stemming from population fluctuations and oscillations in chemical systems. These sections are extensions of material covered in Chapters 6 and 7 respectively.

For a shorter course, any one of the following sequences is suitable: (1) Sections 8.1 and 8.2 (based only on previous material); (2) Sections 8.1 to 8.5

(physiological emphasis); (3) Sections 8.3 and 8.7 (population biology); (4) Sections 8.3, 8.4, 8.6, and 8.8 (mathematical techniques with examples drawn from molecular models).

8.1 NERVE CONDUCTION, THE ACTION POTENTIAL, AND THE HODGKIN-HUXLEY EQUATIONS

One of the leading frontiers of biophysics is the study of neurophysiology, which only several decades ago spawned an understanding of the basic processes underlying the unique electrochemical communication system that constitutes our nervous system. Our brains and every other subsystem in the nervous system are composed of cells called *neurons*. While these vary greatly in size, shape, and properties, such cells commonly share certain typical features (see Figure 8.2). Anatomically, the cell body (*soma*) is the site at which the nucleus and major subcellular structures are located and is the central point from which synthesis and metabolism are coordinated.

A more prominent feature is a long tube-like structure called the *axon* whose length can exceed 1 meter (that is, $\sim 10^5$ times the dimension of the cell body). It is known that the propagation of a nerve signal is electrical in nature; after being initiated at a site called the *axon hillock* (see Figure 8.2) propagates down the length of the axon to terminal branches, which form loose connections (*synapses*) with neighboring neurons. A propagated signal is called an *action potential* (see Figure 8.3).

A neuron has a collection of *dendrites* (branched, "root-like" appendages), which receive incoming signals by way of the synapses and convey them to the soma.

How the detailed electrochemical mechanism operates is a fascinating story that, broadly speaking, is now well understood. It is known that neuronal signals travel *along the cell membrane* of the axon in the form of a local voltage difference across the membrane. A word of explanation is necessary. In the *resting state* the cytoplasm (cellular fluid) inside the axon contains an ionic composition that makes the cell interior slightly negative in potential (-50 mV difference) with respect to the outside (see Figure 8.4). Such a potential difference is maintained at a metabolic expense to the cell by *active pumps* located on the membrane. These continually transport sodium ions (Na^+) to the outside of the cell and convey potassium ions (K^+) inwards so that concentration gradients in both species are maintained. The differences in these and other ionic concentrations across the membrane result in the net electric potential that is maintained across the membrane of the living cell. In this section we take the convention that the voltage v is the potential difference (inside minus outside) for the membrane.

Thinking of the axon as a long electrical cable is a vivid but somewhat erroneous conception of its electrical properties. First, while a current is implicated, it is predominantly made up of ionic flow (not electrons), and its direction is not longitudinal but transverse (into the cell) as shown in Figure 8.5. Second, while a passive cable has fixed resistance per unit length, an axon has an *excitable membrane* whose resistance to the penetration of ions changes as the potential difference v is raised.

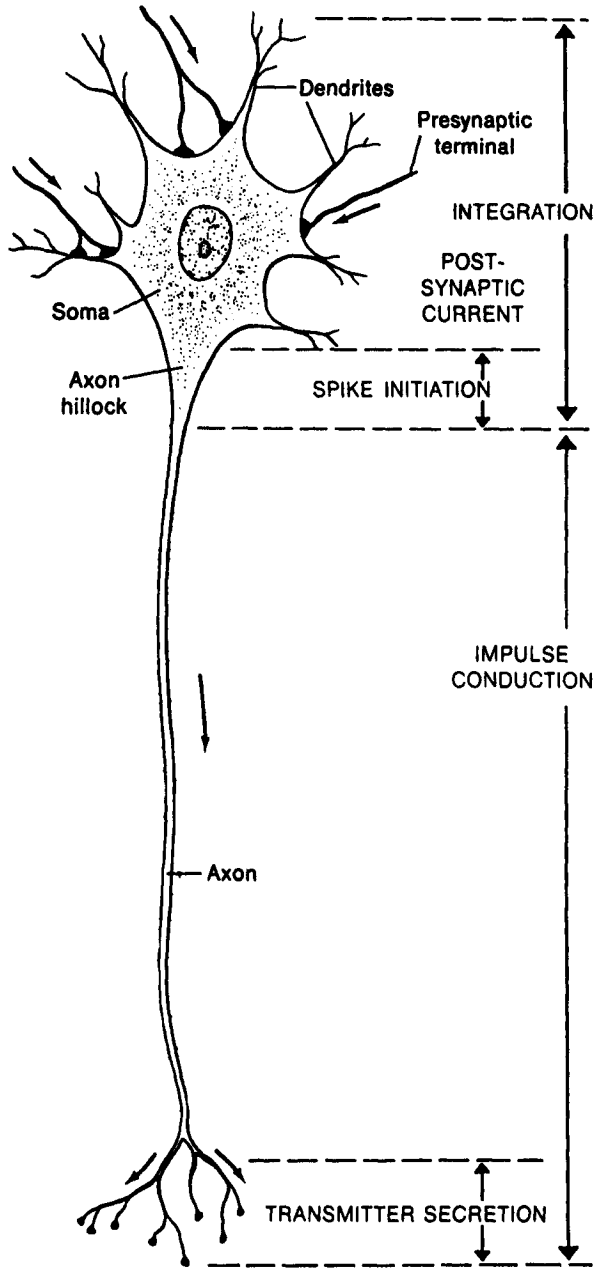

Figure 8.2 *Schematic representation of a neuron showing the cell body (soma) which receives stimuli via the dendrites, the axon along which impulses are conducted, and the terminal branches that form connections (synapses) with other neurons. [From Eckert, R., and Randall, D.* Animal Physiology, *2d edition. W. H. Freeman and Company. Copyright © 1983, p. 179.]*

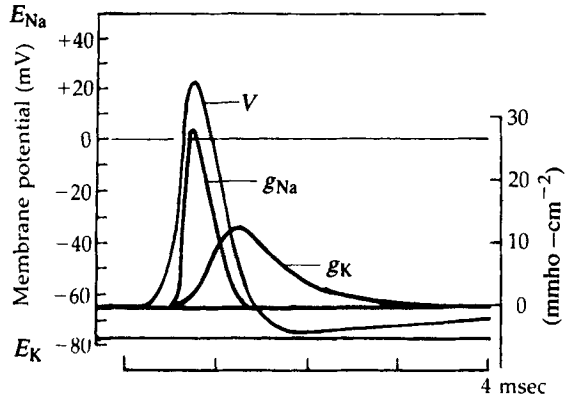

Figure 8.3 *The action potential consists of local changes in voltage across the axon membrane accompanied by changes in the conductivities of the membrane to* Na^+ *and* K^+ *(g_{Na}, g_K) in a time sequence shown here.* (Note: *mho, a unit commonly used for conductance, is equivalent to* $1/ohm$.) *This signal is generally propagated along the neuronal axon from soma to terminal branches. [After Hodgkin and Huxley (1952), from Kuffler, Nicholls, and Martin (1984) p. 151, fig, 13A,* From Neuron to Brain, *2nd edition, by permission of Sinauer Associates Inc.]*

The flow of charged ions across a cell membrane is restricted to specific molecular sites called *pores,* which are sprinkled liberally along the membrane surface. It is now known that many different kinds of pores (each specific to a given ion) are present and that these open and close in response to local conditions including the electrical potential across the membrane. This can be broadly understood in terms of changes in the conformation of the proteins making up these pores, although the biophysical details are not entirely known.

To understand the process by which an action potential signal is propagated, we must look closely at events happening in the immediate vicinity of the membrane. Starting the process requires a *threshold voltage:* the potential difference must be raised to about -30 to -20 mV at some site on the membrane. Experimentally

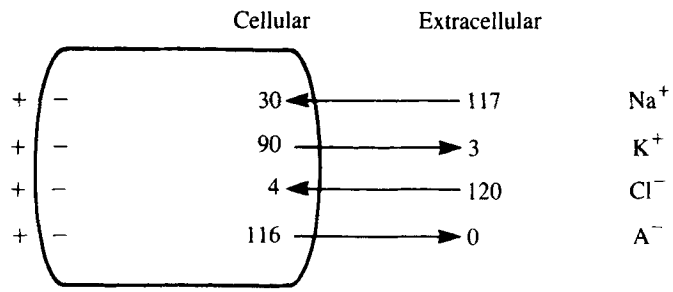

Figure 8.4 *In the resting state, cells have an ionic composition (given here in millimolar units) that differ from that of their environment. Active transport maintains a lower sodium* (Na^+) *and a higher potassium* (K^+) *concentration inside the cell.* Cl^- *and* A^- *represent respectively chlorine ions and other ionic species such as proteins.*

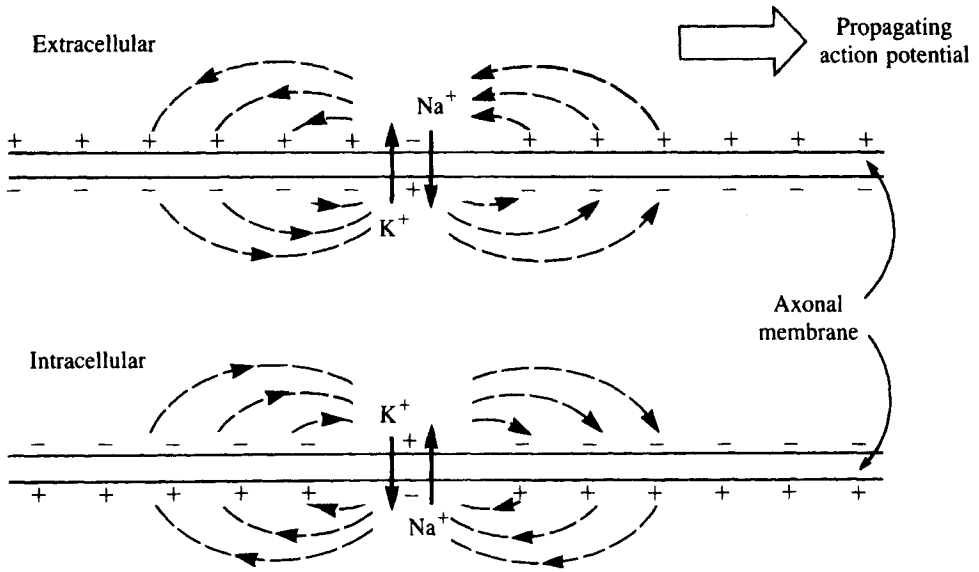

Figure 8.5 *When the axon of a neuron receives a sufficiently large stimulus at some point along its length, the conductivities of the membrane for* Na^+ *and* K^+ *changes. This permits ions to cross the membrane, creating local currents. Since adjacent portions of the membrane are thereby stimulated, the wave of activity known as the action potential can be propagated.*

this can be done by a stimulating electrode that pierces a single neuron. Biologically this happens at the axon hillock in response to an integrated appraisal of excitatory inputs impinging on the soma. As a result of reaching this threshold voltage, the following sequence of events occurs (see Figure 8.6):

1. Sodium channels open, letting a flood of Na^+ ions enter the cell interior. This causes the membrane potential to *depolarize* further; that is, the inside becomes positive with respect to the outside, the reverse of resting-state polarization.
2. After a slight delay, the potassium channels open, letting K^+ *leave* the cell. This restores the original polarization of the membrane, and further causes an overshoot of the negative rest potential.
3. The sodium channels then close in response to a decrease in the potential difference.
4. Adjacent to a site that has experienced these events the potential difference exceeds the threshold level necessary to set in motion step 1. The process repeats, leading to spatial conduction of the spike-like signal. The action potential can thus be transported down the length of the axon without attenuation or change in shape. Mathematically, this makes it a *traveling wave*.

The finer details of this somewhat impressionistic description were uncovered in 1952 in a series of brilliant but painstaking experiments due to Hodgkin, Huxley, and Katz on the giant squid axon, a cell whose axonal diameter is large enough to

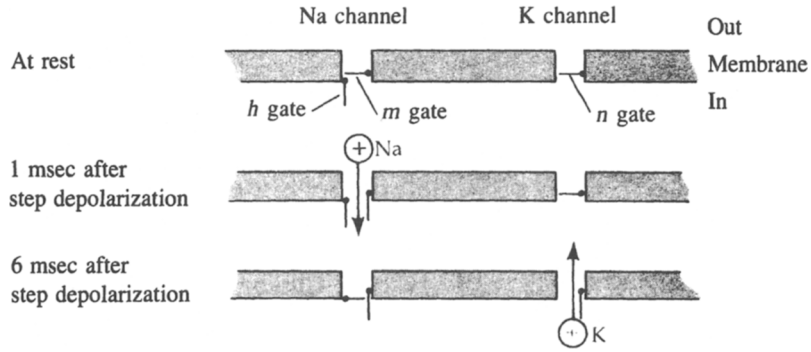

Figure 8.6 *Schematic time sequence depicting the membrane of the axon. Shown are separate pores, governed by gates, for the ions* Na^+ *and* K^+. *At rest the* m *and* n *gates are closed. When a threshold voltage is applied, the* m *gates open rapidly, followed by changes in the other gates. [From Kuffler, Nicholls, and Martin (1984), p. 149, fig. 12.* From Neuron to Brain, *2nd edition, by permission of Sinauer Associates Inc.]*

permit intracellular recording of the voltage by microelectrodes. One technique particularly useful in elucidating the time sequence of ionic conductivities is the *voltage-clamp* experiments. In these, an axon is excised from its cell and its contents are emptied (in a manner akin to squeezing a tube of toothpaste). A thin wire inserted into the hollow axon replaces its cytoplasm and permits an artificially constant voltage to be applied simultaneously along its length. Provided the preparation is kept physiologically active, one can observe a spatially constant but time-varying voltage across the membrane. This voltage has typical action-potential characteristics.

It is further possible to follow the time behavior of the ionic conductivities by a variety of techniques. These include *patch-clamp* experiments, in which single pores are isolated on bits of membrane by suction using fine micropipettes or by selective ionic blocking using agents, such as tetrodotoxin, that bind to ionic pores in a specific way. The detailed structure of some ionic pores is beginning to emerge by a combination of techniques including electron microscopy. (See Figure 8.7.)

With this physiological description we can now discuss the mathematical model that has played a significant role in the advances in neurophysiology. First, a brief review of terminology and properties of an electrical circuit is provided in the box.

The example given in the box, when somewhat modified, can be used to depict electrical properties of the axonal membrane. The idea underlying the approach on which the Hodgkin-Huxley model is based is to use an electric-circuit analog in which physical properties such as ionic conductivities are represented as circuit elements (resistors). The voltage across the membrane thus corresponds to voltage across a collection of resistors, each one depicting a set of ionic pores that selectively permit a limited current of ions. By previous discussions, the resistance (or equivalently, the *conductivities* of such pores) depends on voltage.

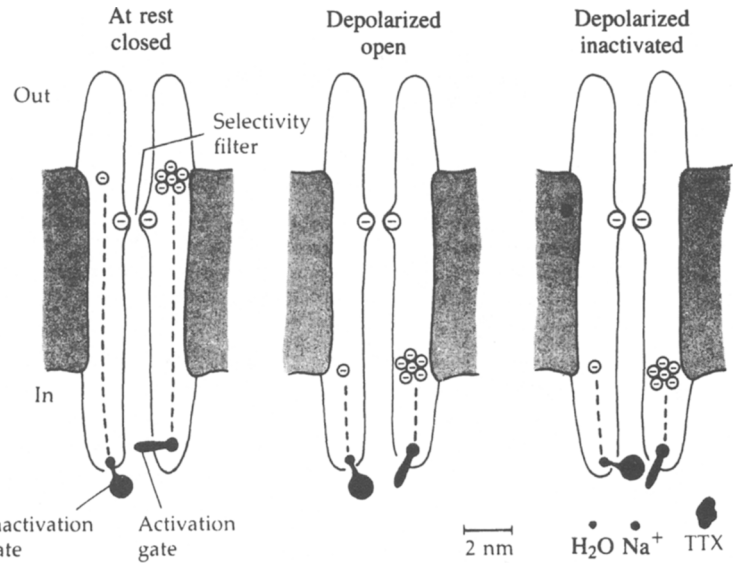

Figure 8.7 *Recent biochemical, electron microscope, and electrophysiological information leads to this schematic sketch of a voltage-sensitive sodium channel. Shown are the activation gates and a constriction that permits selectivity to* Na^+. *Also shown to scale are molecules of water, sodium, and the blocking agent tetrodotoxin (TTX). [From Kuffler, Nicholls, and Martin (1984), p. 156, fig. 15.* From Neuron to Brain, *2nd edition, by permission of Sinauer Associates Inc.]*

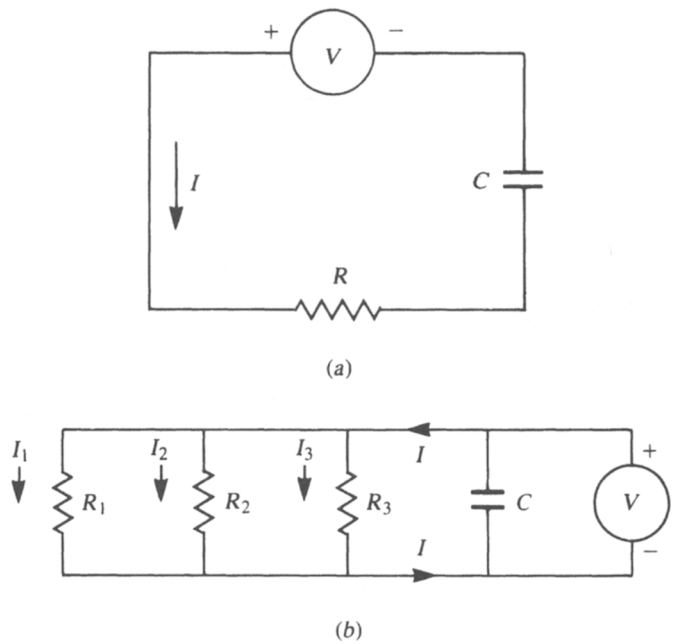

Figure 8.8 *(a) Simple electric circuit. (b) Circuit showing several elements in parallel.*

A Simple Electric Circuit

The following terms are applied in describing a circuit, such as the one shown in Figure 8.8(*a*).

$q(t)$ = the charge (net positive or negative charge carried by particles in the circuit at time t),
$I(t)$ = the current (rate of flow of charge in the circuit) = dq/dt,
$\mathrm{V}(t)$ = the voltage (electromotive force that causes motion of charge; also a measure of the difference in the electrical potential across a given element or set of elements),
R = resistance (property of a material that tends to impede the flow of charged particles),
g = conductance = $1/R$,
C = capacitance (a property of any element that tends to separate physically one group of charged particles from another; this causes a difference in electric potential across the element, called a capacitor).

The following physical relationships hold in a circuit:

1. *Ohm's law:* the voltage drop across a resistor is proportional to the current through the resistor; R or $1/g$ is the factor of proportionality:

$$\mathrm{V}_R(t) = I(t)R = \frac{I(t)}{g}. \tag{2}$$

2. *Faraday's law:* the voltage drop across a capacitor is proportional to the electric charge; $1/C$ is the factor of proportionality:

$$\mathrm{V}_C(t) = \frac{q(t)}{C}. \tag{3}$$

3. *Kirchhoff's law:* the voltage supplied is equal to the total voltage drops in the circuit. For example:

$$\mathrm{V}(t) = \mathrm{V}_R(t) + \mathrm{V}_C(t).$$

4. For several elements in parallel, the total current is equal to the sum of currents in each branch; the voltage across each branch is then the same. In the example shown in Figure 8.8(*b*) the current is

$$I(t) = I_1(t) + I_2(t) + I_3(t) = \frac{\mathrm{V}}{R_1} + \frac{\mathrm{V}}{R_2} + \frac{\mathrm{V}}{R_3}$$
$$= \mathrm{V}(g_1 + g_2 + g_3). \tag{4a}$$

Also,

$$\mathrm{V}(t) = q(t)C. \tag{4b}$$

Differentiating (4b) leads to

$$\frac{d\mathrm{V}}{dt} = \frac{1}{C}\frac{dq}{dt} = \frac{I(t)}{C}. \tag{4c}$$

Thus

$$\frac{dV}{dt} = \frac{V(t)}{C}(g_1 + g_2 + g_3). \tag{4d}$$

In the circuit analog of an axon shown in Figure 8.9, resistance to ionic flow across the membrane is depicted by the conductivities g_K, g_{Na}, and g_L. Resistance to ionic motion inside the axon in an axial direction is represented by longitudinal elements whose resistance per unit length is fixed and much higher than that of the medium surrounding the outer membrane. (The axon has a small radius, which implies greater resistance to flow.) The finite thickness of the membrane is associated with its property of *capacitance*, that is, a separation of charge. We must remember, in looking at this schematic representation, that the axon is cylindrical. Therefore the following modified definitions prove convenient:

$q(x, t)$ = charge density inside the axon at location x and time t (units of charge per unit length),
C = capacitance of the membrane per unit area,
a = radius of the axon,
$I_i(x, t)$ = net rate of exit of positive ions from the exterior to the interior of the axon per unit membrane area at (x, t),
$v(x, t)$ = departure from the resting voltage of the membrane at (x, t).

Then by previous remarks the following relationship is satisfied:

$$q(x, t) = 2\pi aCv(x, t). \tag{5}$$

We shall now assume that a voltage clamp is applied to the axon so that $q = q(t)$, $I_i = I_i(t)$, and $v = v(t)$ and thus all points on the inside of the axon are at the same voltage at any instant. This means that charge will not move longitudinally (there is no force leading to its motion). It can only change by currents that convey ions across the cell membrane. In this case the rate of change of internal charge can be written

$$\frac{dq}{dt} = -2\pi aI_i. \tag{6}$$

The current I_i can be further expressed as a sum of the three currents I_{Na}, I_K, and I_L (sodium, potassium, and all other ions) and related to the potential difference that causes these, as follows:

$$\frac{dq}{dt} = -2\pi a(I_{Na} + I_K + I_L), \tag{7}$$

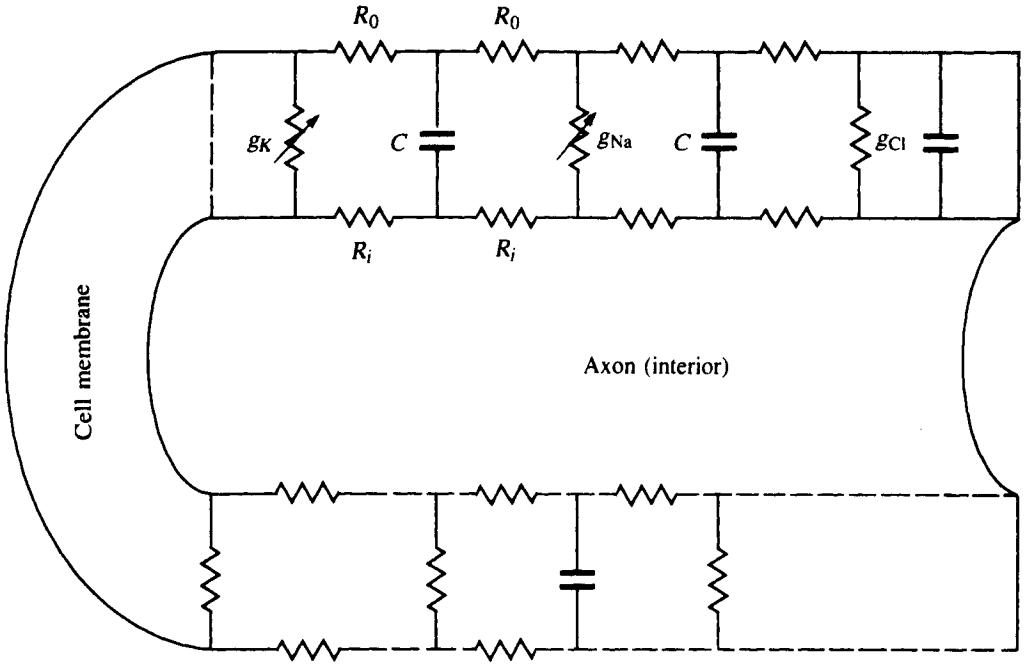

Figure 8.9 *A schematic version of the electric wiring diagram roughly equivalent to the axonal membrane.* g_K, g_{Na}, *and* g_{Cl} *are the voltage-dependent conductivites to* K^+, Na^+, *and* Cl^-; R_i *and* R_0 *represent the resistance of inside and outside environments;* C *depicts the membrane capacitance. (*Note: g_{Cl} *is assumed to be constant.)*

$$I_{Na} = g_{Na}(v - v_{Na}), \tag{8a}$$

$$I_K = g_K(v - v_K), \tag{8b}$$

$$I_L = g_L(v - v_L). \tag{8c}$$

Here v_{Na}, v_K, and v_L represent that part of the resting membrane potential that is due to the contributions of the ions Na^+, K^+, and L (all other mobile species). Furthermore, equation (7) in its entirety may be written in terms of voltage by using equation (5), with the result that

$$\frac{dv}{dt} = -\frac{1}{C}[g_{Na}(v)(v - v_{Na}) + g_K(v)(v - v_K) + g_L(v - v_L)]. \tag{9}$$

It is generally assumed that g_L is independent of v (is constant). At this point Hodgkin, Huxley, and Katz departed somewhat from a straightforward electrical analysis and went on to speculate on a possible mechanism governing the ionic conductivities g_{Na} and g_K. After numerous trial-and-error models, laboriously solved on mechanical calculators, they found it necessary to introduce three variables n, m, and h in the dynamics of the ionic pores. These hypothetical quantities could perhaps be interpreted as concentrations of proteins that must act in concert to open or close a pore. (See Figure 8.6.) However, the equations were chosen to fit the data, not from a more fundamental knowledge of molecular mechanisms.

They defined

$$g_{Na} = \bar{g}_{Na} m^3 h, \tag{10}$$

$$g_K = \bar{g}_K n^4, \tag{11}$$

where $\bar{g}$'s are constant conductivity parameters. They suggested that n, m, and h are voltage-sensitive gate proteins (see Figures 8.6 and 8.7), that obey differential equations in which voltage dependence is described:

$$\frac{dn}{dt} = \alpha_n(v)(1 - n) - \beta_n(v)n, \tag{12a}$$

$$\frac{dm}{dt} = \alpha_m(v)(1 - m) - \beta_m(v)m, \tag{12b}$$

$$\frac{dh}{dt} = \alpha_h(v)(1 - h) - \beta_h(v)h. \tag{12c}$$

In addition, the quantities α_n, α_m, α_h, β_n, β_m, and β_h are assumed to be voltage-dependent as follows:

$$\alpha_m(v) = 0.1(v + 25)(e^{(v+25)/10} - 1)^{-1}, \qquad \beta_m(v) = 4\, e^{v/18}, \tag{13a,b}$$

$$\alpha_h(v) = 0.07\, e^{v/20}, \qquad \beta_h(v) = (e^{(v+30)/10} + 1)^{-1}, \tag{13c,d}$$

$$\alpha_n(v) = 0.01(v + 10)(e^{(v+10)/10} - 1)^{-1}, \qquad \beta_n(v) = 0.125e^{v/80}. \tag{13e,f}$$

The values of other constants appearing in the equations are $\bar{g}_{Na} = 120$, $\bar{g}_K = 36$, and $g_L = 0.3$ mmho cm^{-2}; $v_{Na} = -115$, $v_K = 12$, and $v_L = -10.5989$ mV.

With a physiological system as intricate as the neural axon, it is reasonable to expect rather complicated interactions between variables. In assessing the Hodgkin-Huxley model, we should keep in mind that all but one of its equations were tailored to fit experimental observations. Part of the surprisingly great success of the model lies in its ability to predict fairly accurately the results of many other observations *not* used in formulating the equations. A valid criticism of the model is that the internal variables m, n, and h do not clearly relate to underlying molecular mechanisms; these were, of course, unknown at the time).

The Hodgkin-Huxley equations consist of four coupled ODEs with highly nonlinear terms. For this reason they are quite difficult to understand in an analytic mathematical way. In the next section we explore this model in the elegant way suggested by Fitzhugh. After drawing certain conclusions about the behavior of these equations, we will go on to a much simpler model that captures essential features of the dynamics.

8.2 FITZHUGH'S ANALYSIS OF THE HODGKIN-HUXLEY EQUATIONS

In an elegant paper written in 1960 Fitzhugh set out "to expose to view part of the inner working mechanism of the Hodgkin-Huxley equations." In the year this paper appeared, the three most advanced techniques applied to analysis of nerve conduction models were (1) calculations on a desk calculator (Hodgkin and Huxley's method), (2) Runge-Kutta integration on the digital computers of the late 1950s, (3)

use of the analog computer. Fitzhugh (1960) notes that on the digital computer the solution was very slow, "involving a week or more for a solution, including time for relaying instructions to the operating personnel . . . ." The analog computer used by Fitzhugh was an electronic device consisting of 40 operational amplifiers, six diode function generators, and five servo multipliers. Being much faster than the digital machines then in use, it permitted greater flexibility in experimenting with the equations, but special precautions were necessary to overcome inaccuracies that would have drastically changed the results for reasons that will become clear presently.

Fitzhugh was the first investigator to apply qualitative phase-plane methods to understanding the Hodgkin-Huxley equations. Since this is a system of four coupled equations (in the variables V, m, n, and h), the phase space resides in R^4. To make headway in gaining analytic insight, Fitzhugh first considered the variables that change most rapidly, viewing all others as slowly varying parameters of the system. In this way he derived a reduced two-dimensional system that could be viewed as a phase plane. We follow his method here.

The voltage convention adopted by Fitzhugh $V = v_{out} - v_{in}$ is unfortunately opposite to what subsequently became entrenched in the scientific literature. Thus the first and second quadrants of his phase plane appear reversed relative to the Hodgkin-Huxley model. To avoid possible confusion in conventions we use capital V when referring to Fitzhugh's analysis.

From the Hodgkin-Huxley equations Fitzhugh noticed that the variables V and m change more rapidly than h and n, at least during certain time intervals. By arbitrarily setting h and n to be constant we can isolate a set of two equations which describe a two-dimensional (V, m) phase plane. Plotting the functional relationships representing the nullcline equations ($\dot{m} = 0$ and $\dot{V} = 0$) we obtain Figure 8.10. On this figure the three intersections A, B, and C are steady states; A and C are stable nodes, and B is a saddle point.

The directions of flow in this plane prescribe the following: A small displacement from the "rest state" at A causes a return to this stable node, but a slightly larger deviation (for example, $m = 0$ and $V = -20$ mV) will lead to a large excursion whose final destination is the attracting point C. Note, however, that the nullclines intersect at very small angles at the points A and B. [See enlarged view, Figure 8.11(a).] Consequently there is great sensitivity to any parameter variations that tend to produce small displacements in these curves. This essentially is the effect of incorporating the modulating influence of the other variables. As some critical parameter changes, a displacement is produced, resulting in the following sequence of dynamic behavior:

1. The points A and B approach each other and coalesce.
2. These both vanish as the nullclines separate, leaving a single stable steady state at C. When this transition has occurred, any initial state in the Vm plane is drawn towards C.

Adding a third variable, we might next consider the (V, m, h) equations. A heuristic interpretation given by Fitzhugh is to imagine that as a point traces out a trajectory of Figure 8.10(a) the orbits themselves are "wiggling," so that the phase plane is changing with time. By considering the equation for h, Fitzhugh remarks

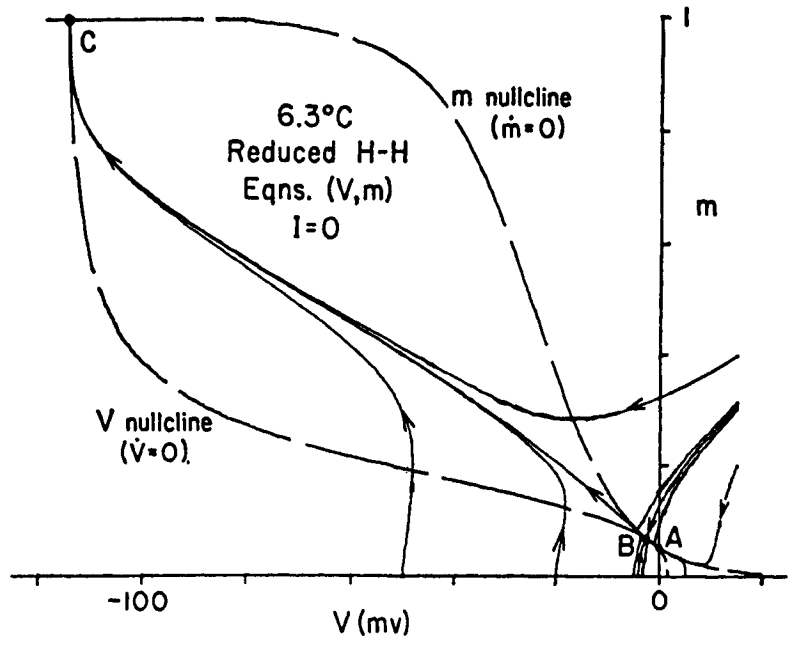

(a)

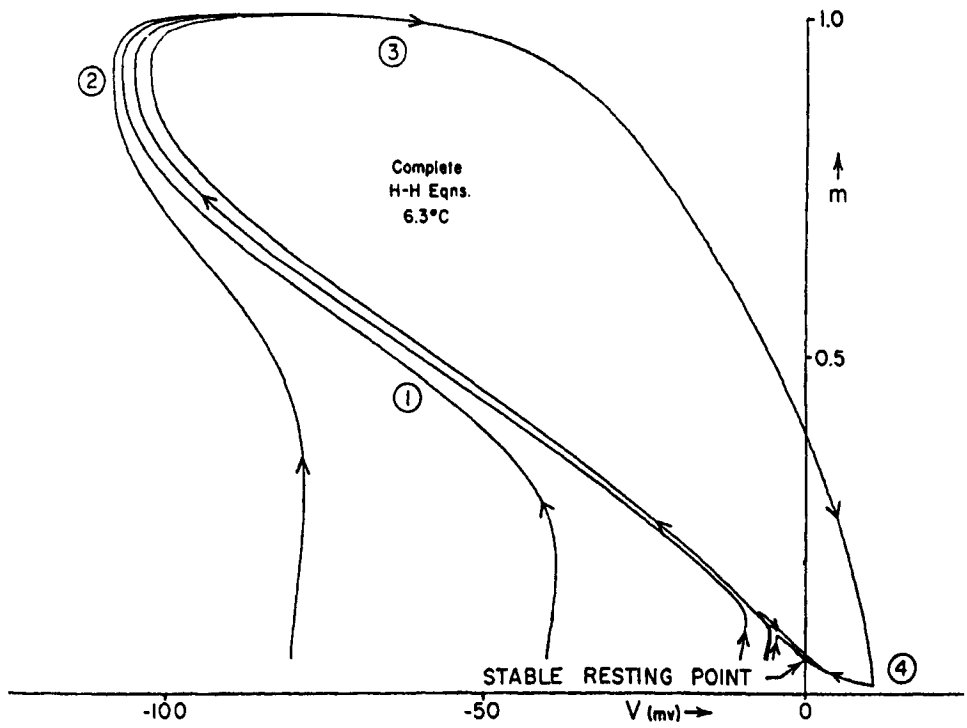

(b)

Figure 8.10 *(a) The reduced phase plane. (b) A projection of the complete Hodgkin-Huxley model on the* Vm *phase plane. [From Fitzhugh (1960), figs. 2 and 9. Reproduced from the* J. Gen. Physiol. *1960, vol. 43, pp. 867–896 by copyright permission of the Biophysical Society.]*

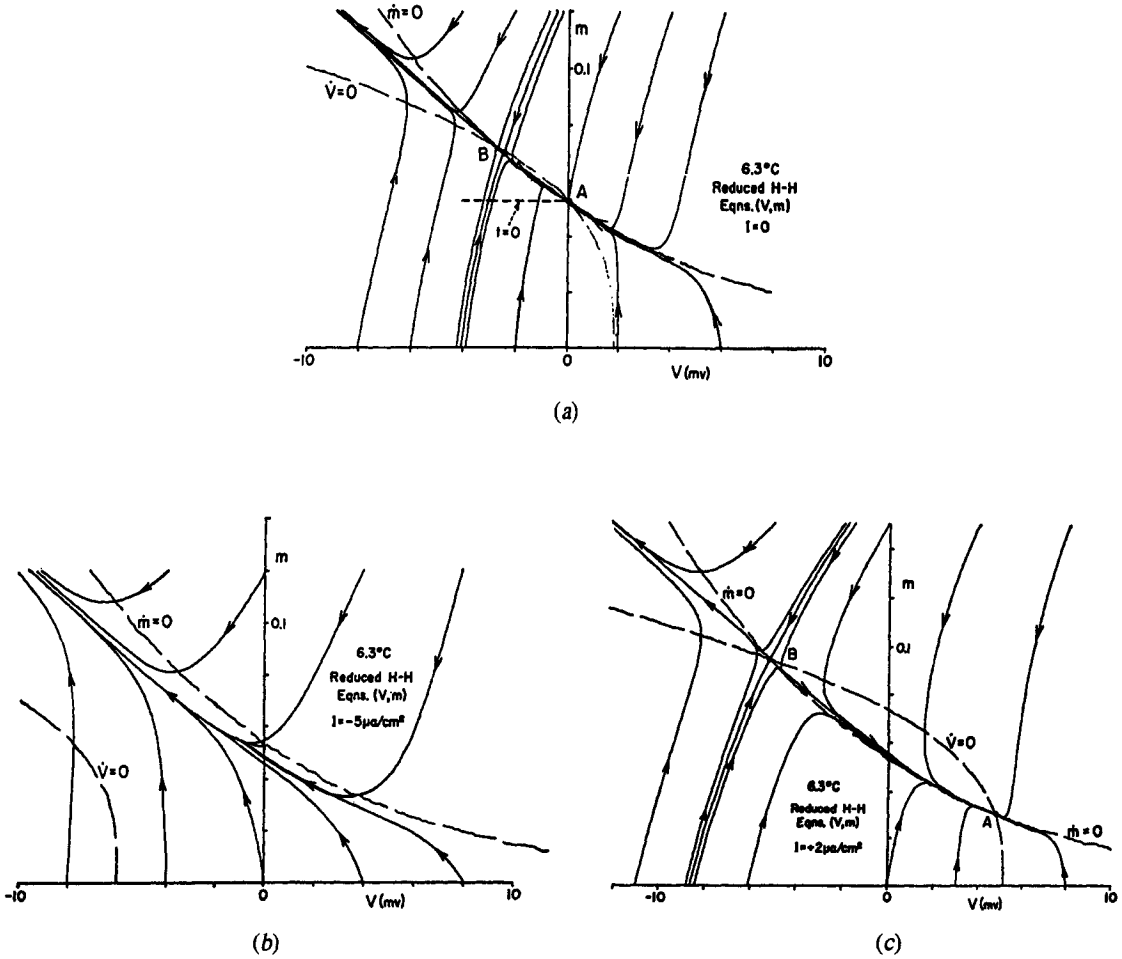

Figure 8.11 *Expanded view of the region of the* Vm *phase plane near the steady states* B *and* A. *(a) In the absence of stimulating current,* A *is a stable node and* B *a saddle point. (b) For super-threshold stimulation,* A *and* B *coalesce and disappear; only* C *will be a steady state. (c) An inhibitory stimulus can cause a greater separation of* A *and* B, *making it less likely that threshold will be exceeded. [From Fitzhugh (1960), figs. 3, 5, and 6. Reproduced from the* J. Gen. Physiol. *1960, vol. 43, pp. 867–896 by copyright permission of the Biophysical Society.]*

that as V becomes negative, h decreases, causing an upwards movement in the V nullcline. For small displacements from rest state A this means that B moves to the left, escaping from the moving phase point, which would then return to A. Larger displacements may initially lie to the left of B, in a region that is initially attracted towards C. However, as the geometry shifts, these points may be overtaken by the moving nullclines and forced back to the rest state of A. Fitzhugh gives more details, described in greater subtlety, in a good expository way.

The entire *Vmhn* phase space was reconstructed and represented by a schematic diagram, a projection into the *Vm* plane. In the complete system there is no saddle point. However, for the variables h and n close to their resting values the system is

essentially equivalent to the reduced (V, m) system in which the point B is a saddle point. As seen in Figure 8.10(b) small deviations from the stable resting point do not lead to excitation, but rather to a gradual return to rest. Larger, above-threshold deviations result in a large excursion through phase space, in which V first increases and finally returns with overshoot to the resting state. Such superthreshold trajectories are the phase-space representations of an action potential. The regions marked on these curves with circled numbers correspond to parts of the physiological response which have been called the (1) regenerative, (2) active, (3) absolutely refractory, and (4) relatively refractory phases.

A familiarity with the Hodgkin-Huxley equations underscores the following:

1. *Excitability:* Above-threshold initial voltage leads to rapid response with large changes in the state of the system.
2. *Stable oscillations:* While not described earlier, the presence of an applied input current represented by an additional term, $I(t)$, on the RHS of equation (9) (e.g. a step function with $I = -10\ \mu\text{A cm}^{-2}$) can lead to the formation of a stable limit cycle in the full model (see Fitzhugh, 1961).

Working with these basic characteristics of the Hodgkin-Huxley model led Fitzhugh to propose a simpler model that gives a descriptive portrait of the neural excitation without direct reference to known or conjectured physiological variables. In preparation for an analysis of his much simpler model we take a mathematical detour to become acquainted with several valuable techniques that will prove useful in a number of upcoming results.

8.3. THE POINCARÉ-BENDIXSON THEORY

As previously mentioned, two-dimensional vector fields and thus also two-dimensional phase planes have attributes quite unlike those of their n-dimensional counterparts. One important feature, on which much of the following theory depends, is the fact that a simple closed curve (for example, a circle) subdivides a plane into two disjoint open regions (the "inside" and the "outside"). This result, known as the *Jordan curve theorem* implies (through a chain of reasoning we shall briefly highlight in Appendix 2 for this chapter) that there are restrictions on the trajectories of a smooth two-dimensional phase flow. As discussed in Chapter 5, a trajectory can approach as its limiting value only one of the following: (1) a critical point, (2) a periodic orbit, (3) a cycle graph (see Figure 8.12), and (4) infinite xy values. A trajectory contained in a *bounded* region of the plane can only fall into cases 1 to 3.

The following result is particularly useful for establishing the existence of periodic orbits.

> ***Theorem 1: The Poincaré-Bendixson Theorem***
> If for $t \geq t_0$ a trajectory is bounded and does not approach any singular point, then it is either a closed periodic orbit or approaches a closed periodic orbit for $t \to \infty$.

Comment: The theorem still holds if we replace $t \geq t_0$ with $t \leq t_0$ and $t \to \infty$ with $t \to -\infty$.

The boxed material outlines properties of a phase plane that are essentially equivalent to the Poincaré-Bendixson theorem and that serve equally well for discovering periodic orbits.

Theorem 2

Suppose the direction field of the system of equations (1a,b) has the following properties:

1. There is a bounded region D in the plane that contains a single repelling steady state and into which flow enters but from which it does not exit. Then the system (1a,b) possesses a periodic solution (represented by a closed orbit lying entirely inside A or D.
2. There is a bounded annular region A in the plane into which flow enters but from which flow does not exit, and A contains no steady states of equations (1a,b).

It is shown in the appendix that the steady state in part 1 can only be an unstable node or focus.

Two other statements outline the stability properties of periodic solutions.

Theorem 3

1. If either of the regions described in theorem 2 contains only a *single* periodic solution, that solution is a stable limit cycle.
2. If Γ_1 and Γ_2 are *two* periodic orbits such that Γ_2 is in the interior of the region bounded by Γ_1 and no periodic orbits or critical points lie between Γ_1 and Γ_2, then one of the orbits must be unstable on the side facing the other orbit.

Much of the theoretical work on proving the existence of oscillatory solutions to nonlinear equations such as (1a,b) rests on identifying regions in the phase plane that have the properties described in theorem 2. We now summarize the Poincaré-Bendixson limit-cycle recipe.

Existence of Periodic Solutions

If you can find a region in the xy phase plane containing a single repelling steady state (i.e. unstable node or spiral) and show that the arrows along the boundary of the region never point outwards, you may conclude that there must be at least one closed periodic trajectory inside the region.

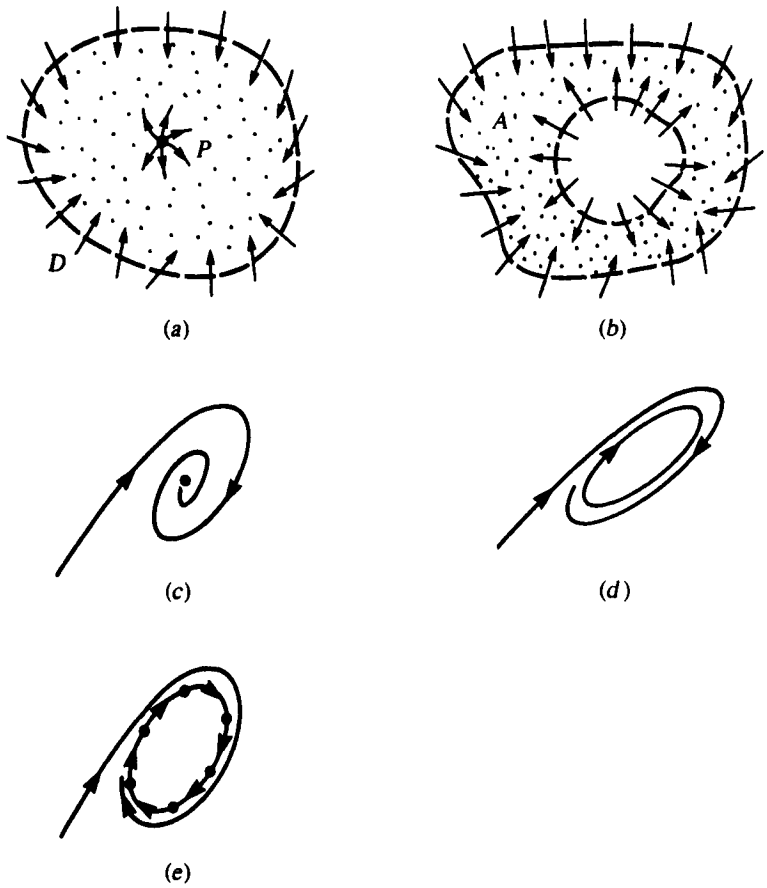

***Figure 8.12** The Poincaré-Bendixson theory prescribes the existence of a limit cycle in two equivalent cases: (a) Flow cannot leave some region* D *that contains an unstable node or focus. (b) Flow is trapped inside an annular region* A *in the* xy *plane. There are three possible fates of a bounded semiorbit: (c) approach to a steady state, (d) approach to a periodic orbit, and (e) approach to a cycle graph.*

An analogous statement corresponding to Figure 8.12(b) can be made. We shall see several examples of the usefulness of the Poincaré-Bendixson theory in this chapter.

The two following criteria are sometimes useful in ruling out the presence of a limit cycle, and for this reason have been called the *negative criteria:*

1. *Bendixson's criterion.* Suppose D is a simply connected region of the plane (that is, D is a region without holes). If the expression $\partial F/\partial x + \partial G/\partial y$ is not identically zero (i.e. is not zero for all (x, y) in D) and does not change sign in D, then there are no closed orbits in this region.
2. *Dulac's criterion:* Suppose D is a simply connected region in the plane, and suppose there exists a function $B(x, y)$, continuously differentiable on D, such that the expression

$$\frac{\partial(BF)}{\partial x} + \frac{\partial(BG)}{\partial y}$$

is not identically zero and does not change sign in D. Then there are no closed orbits in this region.

The proof of Bendixson's criterion is based on Green's theorem and is accessible to students who have had advanced calculus (see appendix to this chapter). Dulac's criterion is an extension that results by substituting BF for F and BG for G in the proof of Bendixson's criterion. For an interesting example of the utility of Dulac's criterion, consider a two-species competition model with carrying capacity κ_i:

$$\frac{dx}{dt} = r_1 x \frac{\kappa_1 - x - \beta_{12} y}{\kappa_1} \tag{14a}$$

$$\frac{dy}{dt} = r_2 y \frac{\kappa_2 - y - \beta_{21} x}{\kappa_2}. \tag{14b}$$

For eliminating limit cycles, Bendixson's criterion fails, but Dulac's criterion succeeds by choosing $B(x, y) = 1/xy$. (See problem 5.) Based on Bendixson's criterion, the following result is readily established.

Corollary of Bendixson's Criterion:

If equations (1a,b) are linear in x and y, then the only possible oscillations are the neutrally stable ones. (Limit cycles can only be obtained with nonlinear equations.)

To understand why this is true, consider the system (1a,b) where $f(x, y) = ax + by$, $G(x, y) = cx + dy$; then $F_x + G_y = a + d$. This is a constant and has a fixed sign. Thus the criterion is only satisfied trivially if $a + d = 0$ in which case the equations would be $dx/dt = by$ and $dy/dt = dx$. Such equations have neutral cycles (not limit cycles), provided b and d have opposite signs.

Comments: Bendixson's negative criterion does not say what happens if the expression $\partial F/\partial x + \partial G/\partial y$ does change sign. (No conclusions can then be drawn about the existence of limit cycles.) In other words, the theorem gives a necessary but *not* a sufficient condition to test.

8.4 THE CASE OF THE CUBIC NULLCLINES

As one application of the Poincaré-Bendixson theorem we examine a rather classical phase-plane geometry that almost invariably leads to the properties of oscillation or excitability. We first discuss a prototype in which one of the nullclines is a simple cubic curve [equation (16)]. As the qualitative analysis will illustrate, this configuration creates the geometry to which the Poincaré-Bendixson theorem applies. An extension to more general S-shaped nullclines will easily follow.

Consider the system of equations

$$\dot{u} = v - G(u), \tag{15a}$$

$$\dot{v} = -u, \tag{15b}$$

where for our prototype we take $G(u)$ to be

$$G(u) = \frac{u^3}{3} - u. \tag{16}$$

We shall postpone a discussion of the motivation underlying these equations and concentrate first on understanding their behavior. One important feature of the function to be exploited presently is that

$$G(u) = -G(-u),$$

that is, G is an *odd* function. Nullclines of this system are the loci of points

$$v = G(u) \qquad \text{(the } u \text{ nullcline)}, \tag{17}$$

$$u = 0 \qquad \text{(the } v \text{ nullcline)}. \tag{18}$$

The term *cubic nullcline* now becomes somewhat more transparent. The shape of the loci given by equation (17) is that of a cubic curve, symmetric about the origin. The two humps to the left and right of the origin also play an important role in the properties of the system. (For this reason the function $G(u) = u^3$ would not be satisfactory; see problem 10 and Figure 8.13.)

Now consider the pattern of flow along these nullclines. The following points can be deduced from the equations:

1. The direction must be "vertical" on the u nullcline and "horizontal" on the v nullcline (since $\dot{u} = 0$ or $\dot{v} = 0$, respectively).
2. Whenever u is positive, v decreases.
3. On the v nullcline, u is zero so that $G(u)$ is also zero. Thus by equation (15a) $\dot{u} = v$, and u will increase when v is positive and decrease when v is negative.

These conclusions are depicted in Figure 8.13(a).

Now consider a trajectory emanating from some arbitrary point $P_0(x_0, y_0)$ in the stippled annulus in Figure 8.13(b). The flow in proximity to the u nullcline will carry it across and towards decreasing u values. After arriving at P_1, the flow drifts horizontally across the v axis and over to the left branch of the cubic curve (P_2). Here a current in the positive v direction conveys the point to P_3 and then back across the top of the hump and into the positive quadrant. From the construction in the diagram it is further evident that the direction of flow is everywhere *into* or parallel to the boundary of the annular region, indicating that once a trajectory has entered the region, it is forever trapped. There are no steady-state points in A, and A is bounded. By the Poincaré-Bendixson theorem we can conclude that there is a limit-cycle trajectory inside this region.

Furthermore, it is possible to shrink the thickness of A to an arbitrarily fine region and draw similar conclusions. In particular, this means that we can dismiss the

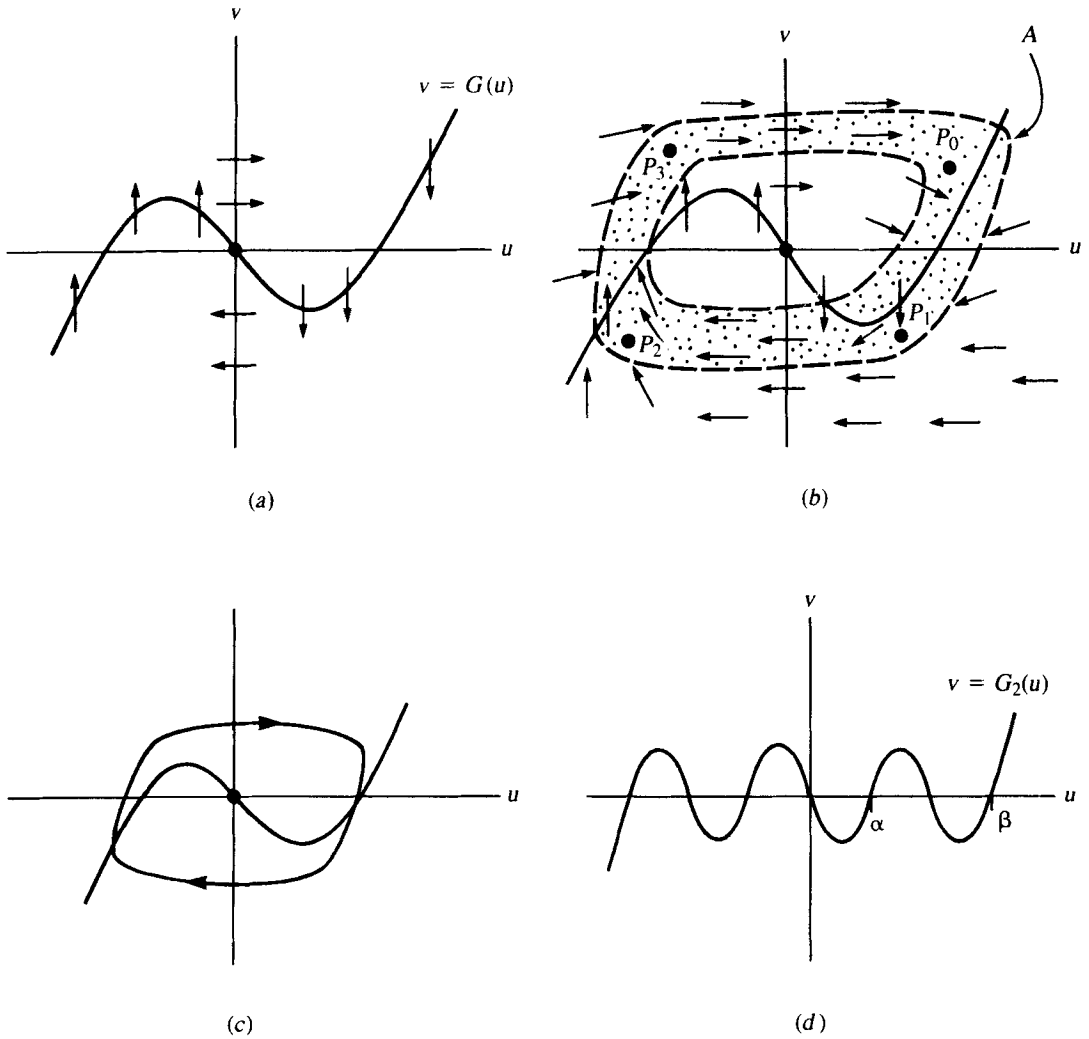

Figure 8.13 *Flow along cubic nullclines described by equations (15) and (16); (b) an annular region* A *that traps flow in the* uv *plane; (c) a limit cycle oscillation contained in the region* A*; (d) more general shapes of the function* G *that lead to similar results.*

possibility that there is more than one limit cycle in the dynamical system. (See Problem 10.)

We have chosen a particular example in which the form of the equations leads to certain specific features: (steady state at (0, 0), flow symmetric with respect to the origin, and one nullcline along the y axis). These features can be changed somewhat without losing the main dynamic features of the system. More generally, a broader class known as the *Lienard equations* exhibit similar behavior. Sometimes written as the following single equation,

$$\frac{d^2u}{dt^2} + g(u)\frac{du}{dt} + u = 0, \tag{19}$$

it can be shown to be equivalent to the system of (15a,b), where

$$G(u) = \int_0^u g(s)\,ds. \tag{20}$$

Then the following properties of $G(u)$ lead to a generalized cubic that results in essentially identical conditions:

1. $G(u) = -G(-u)$ (thus $G(u)$ is an odd function).
2. $G(u) \to \infty$ for $u \to \infty$ (the right and left branches of G extend to $+\infty$ and $-\infty$) and for some positive β, $G(u) > 0$ and $dG/du > 0$ whenever $u > \beta$; (G is eventually positive and monotonically increasing).
3. For some positive α, $G(\alpha) = 0$ and $G(u) < 0$ whenever $u < \alpha$. (G is negative for small positive u values).

Condition 1 means that all trajectories will be symmetric about the origin. Condition 2 is necessary to cause the flow to be trapped or confined to the given annulus. Condition 3 means that the steady state at (0, 0) is unstable. (Details are investigated in problem 11.) An example of a "bumpy" function satisfying these conditions is shown in Figure 8.13(*d*). It can be rigorously established (with reasoning similar to that used earlier) that such conditions guarantee that the system of equations (15) (or the single equation 19) admits a nontrivial periodic solution, that is, a limit cycle. In the particular case where $\alpha = \beta$, as in the example we have analyzed, there is indeed a single periodic orbit that is asymptotically stable. Rigorous proof and further details may be found in Hale (1980), (p. 57–63).

The example used as a prototype in this section is called the *Van der Pol oscillator,* sometimes written in the form

$$\ddot{u} - k(1 - u^2)\dot{u} + u = 0 \qquad (k > 0). \tag{21}$$

(See problem 12.) Van der Pol first used it in 1927 to represent an electric circuit containing a nonlinear element (a triode valve whose resistance depends on the applied current). Even then, van der Pol realized the parallel between this circuit and certain biological oscillations such as the heart beat. For large values of the constant k, the corresponding system of equations

$$\epsilon\dot{u} = v - G(u), \tag{22a}$$

$$\dot{v} = -u\epsilon, \tag{22b}$$

contains a small parameter $\epsilon = 1/k$. (Recall that this can be exploited in calculating approximate solutions using techniques of asymptotic expansions. See problem 12 for a taste of the idea.) The solutions to this small-parameter system are called *relaxation oscillations* for the following reasons: as long as v is close to $G(u)$ (that is, in vicinity of the cubic curve), $\dot{u}$ and $\dot{v}$ both change rather slowly. When the trajectory

departs from this curve, $\dot{u} = [v - G(u)]/\epsilon$ is quite large. The horizontal progression across from P_1 to P_2 is thus rapid. A plot of $u(t)$ reveals a succession of time intervals in which u changes slowly followed by ones in which it changes more rapidly.

Models related to van der Pol's oscillator have been important in many physical settings and, as we shall see, have also been valuable in describing oscillating biological systems. (A example of an application to the heart-beat cycle is discussed in Jones and Sleeman, 1983.) More generally, the idea underlying s-shaped nullclines has been exploited in a variety of models for excitable and oscillatory phenomena. Figures 8.14 to 8.17 are a sampling drawn from the literature, and Section 8.5 deals in greater detail with one particular application in the study of neural signals.

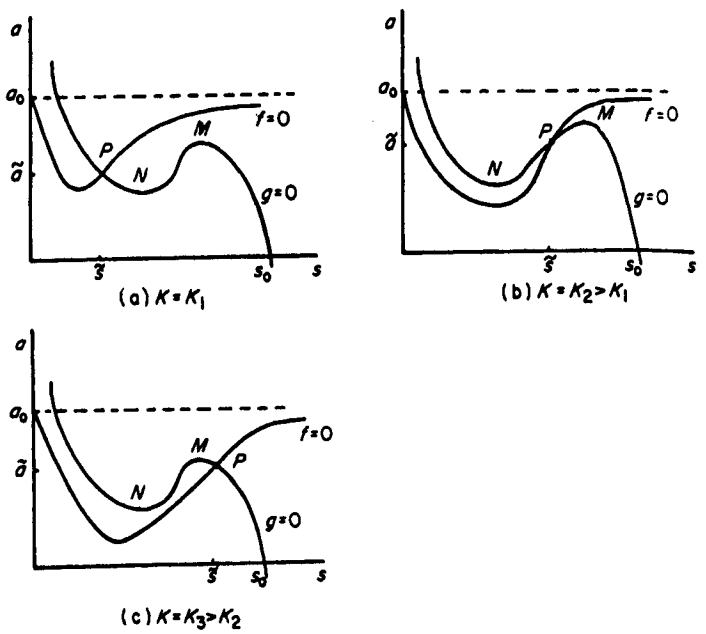

Figure 8.14 *Several regimes of behavior in a model for substrate inhibition with* S*-shaped nullclines.* s *and* a *represent substrate and cosubstrate. Their chemical kinetics are represented by the equations*

$$\frac{ds}{dt} = g(s, a), \qquad \frac{da}{dt} = f(s, a)$$

where

$$g = s_0 - s - \frac{\rho s a}{1 + s + Ks^2},$$

$$f = \alpha(a_0 - a) - \frac{\rho s a}{1 + s + Ks^2}.$$

K *is the inhibition parameter,* α, ρ, a_0 *and* s_0 *are constants (see details in the original reference.)* M *and* N *represent the maximum and minimum points along the nullcline* g = 0, *and* P *is the steady state. The transition* a) → b) → c) *is for decreasing* K*-values. [From Murray (1981), fig. 2, p. 168.* J. Theor. Biol., *88, 161–199. Reprinted by permission of Academic Press Inc. (London)]*

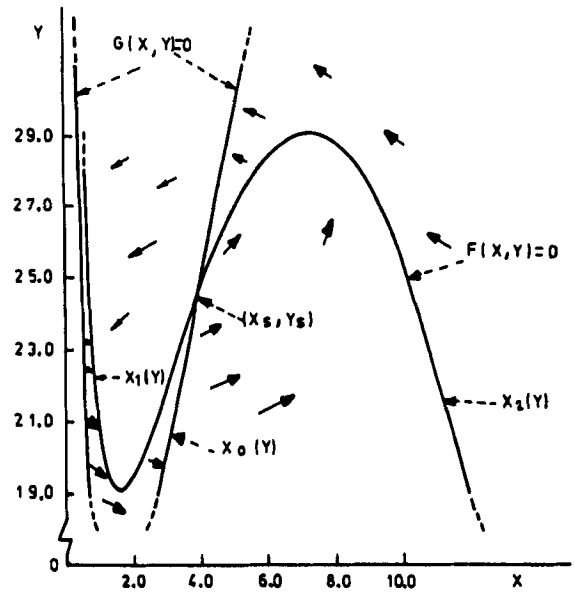

Figure 8.15 *A vector field and cubic nullclines in a model for respiration in a bacterial culture. The nutrient* x *and oxygen* y *are assumed to satisfy the equations*

$$\frac{dx}{dt} = B - x - \frac{xy}{1 + qx^2} = F(x, y),$$

$$\frac{dy}{dt} = A - \frac{xy}{1 + qx^2} = G(x, y).$$

Typical parameter values for stable oscillations are

$A = 11.0,\ B = 19.4,\ q = 0.5.$

[From Fairen and Velarde (1979). Fig. 3, p. 152, J. Math. Biol., *8, 147–157, by permission of Springer-Verlag.]*

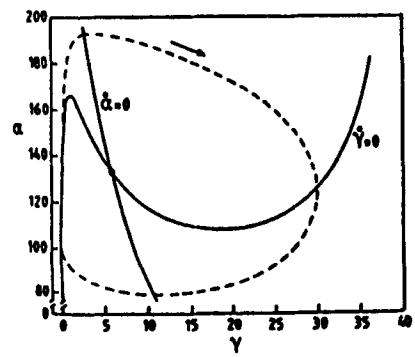

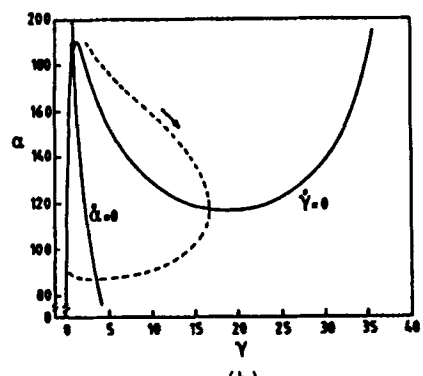

Figure 8.16 *(a) Limit-cycle oscillations, and (b) excitability on suprathreshold perturbation, in a two-variable system derived from equations for a cyclic-AMP signaling system devised by Goldbeter and Segel (1977). The original equations are*

$$\frac{d\alpha}{dt} = v - \sigma\Phi \qquad \text{(intracellular ATP)},$$

$$\frac{d\beta}{dt} = q\sigma\Phi - k_t\beta \qquad \text{(intracellular CAMP)},$$

$$\frac{d\gamma}{dt} = \frac{k_t\beta}{h} - k_s\gamma \qquad \text{(extracellular CAMP)},$$

α, β *and* γ *represent dimensionless metabolic concentrations and*

$$\Phi = \frac{\alpha(1 + \alpha)(1 + \gamma)^2}{L + (1 + \alpha)^2(1 + \gamma)^2} \qquad \text{(allosteric kinetics of adenylate cyclase)}$$

is a chemical kinetic term depicting enzyme—receptor interactions. See Segel (1984) for a simplified model and definitions of parameters. [From Goldbeter and Martiel (1983). A critical discussion of plausible models for relay and oscillation of cyclic AMP in dictyostelium cells, in Rhythms in Biology and other Fields of Application Lecture Notes in Biomath, *vol. 49, pp 173–178. Reprinted with author's permission.]*

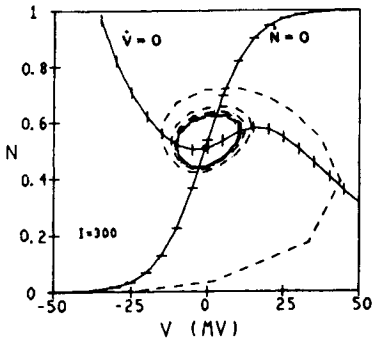

(a)

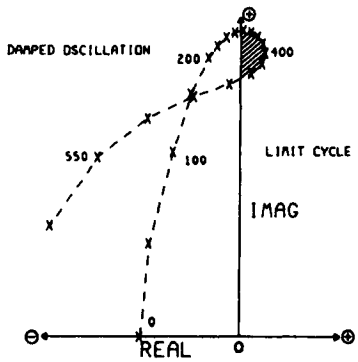

(b)

Figure 8.17 *(a) S-shaped nullclines in a model for voltage oscillations in the barnacle giant muscle fiber. Shown is a limit cycle in a reduced* V, N *system (*V = *voltage and* N = *fraction of open* K^+ *channels);* V *satisfies an equation like (9), and* N *is given by*

$$\frac{dN}{dt} = \lambda_N(V)(N_\infty(V) - N),$$

where

$$N_\infty = \frac{1}{2}\left(1 + \tanh\frac{v - v_3}{v_4}\right).$$

(b) The eigenvalues of the linearized system change as the current is increased and cross the imaginary axis twice. [From Morris and Lecar (1981), figs. 7 and 8. Reproduced from the Biophysical Journal *(1981) vol 35, 193–213, by copyright permission of the Biophysical Society.]*

Conclusions

A system of equations (1a,b) in which one of the nullclines $F(x, y) = 0$ or $G(x, y) = 0$ is an S-shaped curve can give rise to *oscillations* provided the steady state on this curve is unstable.

When the steady state is stable, the system may exhibit a somewhat different behavior called *excitability*. We discuss this property further in Section 8.5.

8.5 THE FITZHUGH-NAGUMO MODEL FOR NEURAL IMPULSES

In Section 8.2 we followed an analysis of the Hodgkin-Huxley model published by Fitzhugh in the biophysical literature in 1960. The elegance of applying phase-plane methods and reduced systems of equations to this rather complicated problem should not be underestimated. (Similar ideas are used in more recent examples; see Morris and Lecar, 1981.)

Using such analysis, Fitzhugh was able to explain the occurrence of thresholds in the Hodgkin-Huxley model of neural excitation. The analysis was, however, less instructive in demonstrating causes of *repetitive impulses* (a sequence of action potentials in the neuron) because here the interactions of all four variables—V, m, h, and n—were important [see equations (9) to (12).] A greater reliance on numerical, rather than analytic techniques was thus necessary.

In a succeeding paper published in 1961, Fitzhugh proposed to demonstrate that the Hodgkin-Huxley model belongs to a more general class of systems that exhibit the properties of excitability and oscillations. As a fundamental prototype, the van der Pol oscillator was an example of this class, and Fitzhugh therefore used it (after suitable modification). A similar approach was developed independently by Nagumo et al. (1962) so the following model has subsequently been called the Fitzhugh-Nagumo equations.

To avoid misunderstanding, it should be emphasized that the main purpose of the model is not to portray accurately quantitative properties of impulses in the axon. Indeed, the variables in the equations have somewhat imprecise meanings, and their interrelationship does not correspond to exact physiological facts or conjectures. Rather, the system is meant as a simpler paradigm in which one can exhibit the sorts of interactions between variables that lead to properties such as excitability and oscillations (repetitive impulses).

Fitzhugh proposed the following equations:

$$\frac{dx}{dt} = c\left[y + x - \frac{x^3}{3} + z(t)\right], \tag{23a}$$

$$\frac{dy}{dt} = -\frac{x - a + by}{c}. \tag{23b}$$

In these equations the variable x represents the excitability of the system and could be identified with voltage (membrane potential in the axon); y is a recovery variable, representing combined forces that tend to return the state of the axonal membrane to rest. Finally, $z(t)$ is the applied stimulus that leads to excitation (such as input current). In typical physiological situations, such stimuli might be impulses, step functions, or rectangular pulses. It is thus of interest to explore how equations (23a,b) behave when various functions $z(t)$ are used as inputs. Before addressing this question we first take $z = 0$ and analyze the behavior of the system in the xy phase plane.

In order to obtain suitable behavior, Fitzhugh made the following assumptions about the constants a, b, and c:

$$1 - \frac{2b}{3} < a < 1, \qquad 0 < b < 1, \qquad b < c^2, \tag{24}$$

Inspection reveals that when $z = 0$, nullclines of equations (23a,b) are given by the following loci:

$$y = \frac{x^3}{3} - x \qquad (\dot{x} = 0, \text{ the } x \text{ nullcline}), \tag{25}$$

$$y = \frac{a - x}{b} \qquad (\dot{y} = 0, \text{ the } y \text{ nullcline}). \tag{26}$$

The humps on the cubic curve are located at $x = \pm 1$.

We shall not explicitly solve for the steady state of this system, which satisfies the cubic equation

$$\frac{x^3}{3} + x\left(\frac{1}{b} - 1\right) = \frac{a}{b}. \tag{27}$$

However, the conditions given by equation (24) on the parameters guarantee that there will be a *single* (real) steady-state value $(\bar{x}, \bar{y})$ located just beyond the negative hump on the cubic x nullcline, at its intersection with the skewed y nullcline, as shown in Figure 8.18.

Calculating the Jacobian of equations (23) leads to

$$\mathbf{J} = \begin{pmatrix} (1 - \bar{x}^2)c & c \\ \dfrac{-1}{c} & \dfrac{-b}{c} \end{pmatrix} \tag{28}$$

(problem *g*). Thus, by writing the characteristic equation in terms of $\bar{x}$, we obtain the quadratic equation

$$\lambda^2 + \left[\frac{b}{c} - (1 - \bar{x}^2)c\right]\lambda + [1 - (1 - \bar{x}^2)b] = 0. \tag{29}$$

The steady state will therefore be stable provided that

$$-\left[\frac{b}{c} - (1 - \bar{x}^2)c\right] < 0, \tag{30a}$$

$$1 - (1 - \bar{x}^2)b > 0. \tag{30b}$$

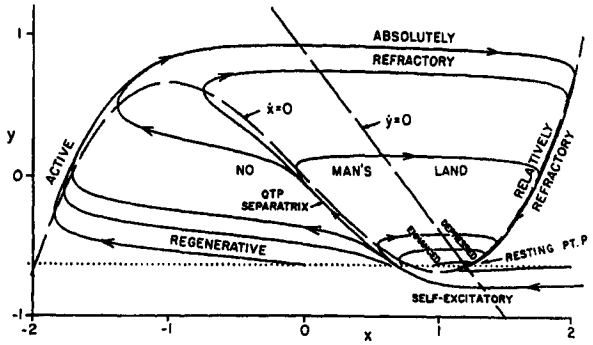

(a)

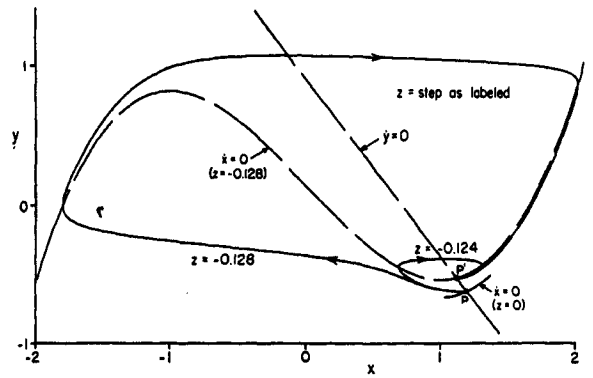

(b)

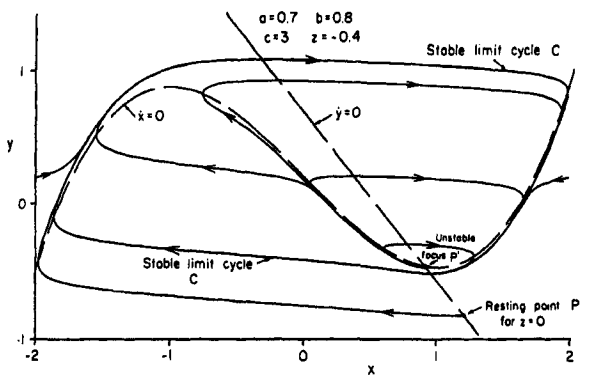

(c)

Figure 8.18 *Fitzhugh's model [equations 23a,b] leads to the basic phase-plane behavior shown in (a) for* z = 0. *(See text for an interpretation of* x, y, *and* z. *The resting point corresponds to the rest state of the neuron. (b) In the presence of a step input of weak current* (z = −0.128) *the system undergoes excitation analogous to a single action potential. (c) For a step input of stronger current, an infinite train of impulses (repetitive action potentials) are generated. [From Fitzhugh (1961), figs. 1, 3, and 5. Reproduced from the* Biophysical Journal, *1961, vol 1, pp 445–466, by copyright permission of the Biophysical Society.]*

Note that these conclusions are not affected if z in equation (23a) is nonzero. Since $b < 1$ and $b < c^2$, it may be shown (problem g) that the steady state is stable for all values of $\bar{x}$ that are not in the range

$$-\gamma \leq \bar{x} \leq \gamma, \tag{31}$$

where $\gamma = (1 - b/c^2)^{1/2}$ is a positive number whose magnitude is smaller than 1. The geometry shown in Figure 8.18 tells us that if the y nullcline were to intersect the cubic x nullcline somewhere on the middle branch between the two humps, the steady state would be unstable.

We next consider the behavior of the *stimulated* neuron, described by equations (23a,b) with a nonzero stimulating current $z(t)$. A particularly simple set of stimuli might consist of the following:

1. A step function $z = 0$ for $t < 0$; $z = i_0$ for $t \geq 0$).
2. A pulse ($z = i_0$ for $0 \leq t \leq t_0$; $z = 0$ otherwise.
3. A constant current $z = i_0$.

For as long as $z = i_0$, the configuration of the x nullcline is given by the equation

$$y = \frac{x^3}{3} - x + i_0. \tag{32}$$

This cubic curve has been shifted in the positive y direction if i_0 is positive and in the opposite direction if i_0 is negative. Let S^* represent the intersection of (32) with the y nullcline, S^0 the intersection of (25) with the y nullcline, and S the instantaneous state of the system. Thus S^* and S^0 are the steady states of the stimulated and unstimulated system, respectively and $S = (x(t), y(t))$.

At the instant a stimulus is applied, $S = S^0$ is no longer a rest state, since the steady state has shifted to S^*. This means that S will change, tracing out some trajectory in the xy plane. The following possibilities arise:

1. If i_0 is very small, S^* will be close to S^0, on the region of the cubic curve for which steady states are stable and $S = (x(t), y(t))$ will be attracted to S^* without undergoing a large displacement.
2. If i_0 is somewhat larger, S^* may still be in the stable regime, but a more abrupt dynamics could ensue: in particular, if S falls beyond the separatrix shown in Figure 8.18(a), the state of the system will undergo a large excursion in the xy plane before settling into the attracting steady state S^*.

Such cases represent a single action-potential response that occurs for superthreshold stimuli. (See Figure 8.3.) This type of behavior, in which a steady state is attained only after a long detour in phase space, is typical of *excitable systems*. As we have seen, it is also a property intimately associated with systems in which one or both of the nullclines have the S shape (also referred to sometimes as N shape or z shape) similar to that of the cubic curve.

3. For yet larger i_0, S^* will fall into the middle branch of the cubic curve so that it is no longer stable. In this case the situation discussed in Section 8.5 occurs and a stable, closed, periodic trajectory is created. All points, and in particular

S, will undergo cyclic dynamics, approaching ever closer to the stable limit cycle. This behavior corresponds to *repetitive firing* of the axon, which results when a step stimulus of sufficiently high intensity is applied.

In all of these cases, when the applied stimulus is removed (at $z = 0$), S^0 becomes an attracting rest state once more; the repetitive firing ceases, and the excited state eventually returns to rest.

With a few masterful strokes, Fitzhugh has painted a *caricature* of the behavior of neural excitation. His model is not meant to accurately portray the physiological mechanisms operating inside the axonal membrane. Rather, it is a behavioral paradigm, phrased in terms of equations that are mathematically tractable. As such it has played an important role in leading to an understanding of the nature of excitable systems and in studying more complicated models of the action potential that include the effect of spatial propagation in the native (nonclamped) axon.

8.6 THE HOPF BIFURCATION

A further diagnostic tool that can help in establishing the existence of a limit-cycle trajectory is the *Hopf bifurcation theorem*. It is quoted widely, applied in numerous contexts, and for this reason merits discussion.

Subject to certain restrictions, this theorem predicts the appearance of a limit cycle about any steady state that undergoes a transition from *a stable to an unstable focus* as some parameter is varied. The result is local in the following sense: (1) The theorem only holds for parameter values close to the *bifurcation value* (the value at which the just-mentioned transition occurs). (2) The predicted limit cycle is close to the steady state (has a small diameter). (The Hopf bifurcation does not specify what happens as the *bifurcation parameter* is further varied beyond the immediate vicinity of its critical bifurcation value.)

In the following box the theorem is stated for the case $n = 2$. A key requirement corresponding to our informal description is that the given steady state be associated with *complex* eigenvalues whose real part changes sign (from $-$ to $+$). In popular phrasing, such eigenvalues are said to "cross the real axis." To recall the connection between complex eigenvalues and oscillatory trajectories, consider the discussion in Section 5.7 (and in particular, Figure 5.12 of Chapter 5).

Advanced mathematical statements of this theorem and its applications can be found in Marsden and McCracken (1976). Odell (1980) and Rapp (1979) give good informal descriptions of this result that are suitable for nonmathematical readers.

One of the attractive features of the Hopf bifurcation theorem is that it applies to larger systems of equations, again subject to certain restrictions. This makes it somewhat more applicable than the Poincaré-Bendixson theorem, which holds only for the case $n = 2$.

The Hopf Bifurcation Theorem for the Case n = 2

Consider a system of two equations that contains a parameter γ.

$$\frac{dx}{dt} = f(x, y; \gamma), \tag{33a}$$

$$\frac{dy}{dt} = g(x, y; \gamma). \tag{33b}$$

The usual differentiability and continuity assumptions are made about f and g as functions of x, y, and γ (see Chapter 5). Suppose that for each value of γ the equations admit a steady state whose value may depend on γ, that is, $(\bar{x}(\gamma), \bar{y}(\gamma))$. Consider the Jacobian matrix evaluated at the parameter-dependent steady state:

$$\mathbf{J}(\gamma) = \begin{pmatrix} \frac{\partial f}{\partial x} & \frac{\partial f}{\partial y} \\ \frac{\partial g}{\partial x} & \frac{\partial g}{\partial y} \end{pmatrix}_{(\bar{x}, \bar{y})} \tag{34}$$

Suppose eigenvalues of this matrix are $\lambda(\gamma) = a(\gamma) \pm b(\gamma)i$. Also suppose that there is a value γ^*, called the bifurcation value, such that $a(\gamma^*) = 0$, $b(\gamma^*) \neq 0$, and as γ is varied through γ^*, the real parts of the eigenvalues change signs ($da/d\gamma \neq 0$ at $\gamma = \gamma^*$).

Given these hypotheses, the following possibilities arise:

1. At the value $\gamma = \gamma^*$ a center is created at the steady state, and thus infinitely many neturally stable concentric closed orbits surround the point $(\bar{x}, \bar{y})$.
2. There is a range of γ values such that $\gamma^* < \gamma < c$ for which a *single* closed orbit (a limit cycle) surrounds $(\bar{x}, \bar{y})$. As γ is varied, the diameter of the limit cycle changes in proportion to $|\gamma - \gamma^*|^{1/2}$. There are no other closed orbits near $(\bar{x}, \bar{y})$. Since the limit cycle exists for γ values *above* γ^*, this phenomenon is known as a *supercritical bifurcation*.
3. There is a range of values such that $d < \gamma < \gamma^*$ for which a conclusion similar to case 2 holds. (The limit cycle exists for values below γ^*, and this is termed a *subcritical bifurcation*.)

Figure 8.19 illustrates what can happen close to a bifurcation value γ^* (in the case $n = 2$). Here the xy phase plane has been drawn for several values of the parameter γ. In Figure 8.19(a) observe that as γ increases from small values through γ^* and up to $\gamma = c$ the steady state changes from a stable focus to an unstable focus. A stable limit cycle appears at γ^*, and its diameter grows as indicated by the parabolic envelope. This succession, called a supercritical bifurcation, is often represented schematically by the bifurcation diagram of Figure 8.19(c).

In Figure 8.19(b) an unstable limit cycle accompanies the stable focus until γ increases beyond γ^* and disappears. This type of transition, called a *subcritical* bifurcation, is represented by Figure 8.19(d). (Recall that in bifurcation diagrams solid

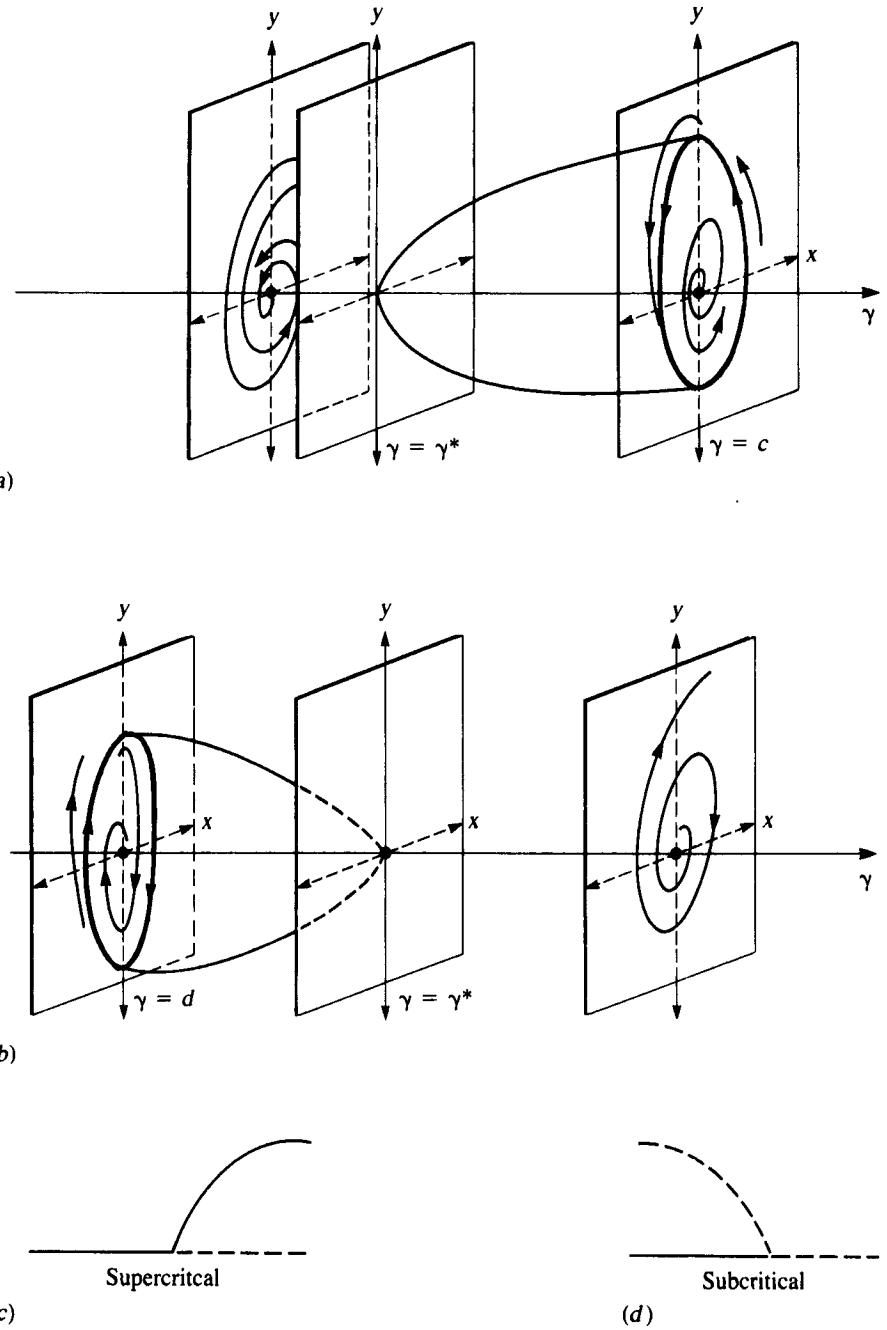

Figure 8.19 *Limit cycles can appear close to a bifurcation value γ^* of some parameter γ when a transition from stable to unstable focus occurs at a steady state (a) A supercritical bifurcation occurs for $\gamma > \gamma^*$. (b) A subcritical bifurcation occurs for $\gamma < \gamma^*$. The Hopf bifurcation theorem gives conditions that guarantee the existence and stability properties of such limit-cycle solutions. It has been assumed that the steady state is stable when $\gamma < \gamma^*$ and unstable when $\gamma > \gamma^*$. (c, d) The bifurcation diagrams summarize this parameter dependence.*

The Hopf Bifurcation Theorem for the Case $n > 2$

Consider a system of n equations in n variables,

$$\frac{d\mathbf{x}}{dt} = \mathbf{F}(\mathbf{x}, \gamma),$$

where

$$\mathbf{x} = (x_1, x_2, \ldots, x_n),$$
$$\mathbf{F} = (f_1(\mathbf{x}; \gamma), f_2(\mathbf{x}; \gamma), \ldots, f_n(\mathbf{x}; \gamma)),$$

with the appropriate smoothness assumptions on f_i which are functions of the variables and a parameter γ. If $\bar{\mathbf{x}}$ is a steady state of this system and linearization about this point yields n eigenvalues

$$\lambda_1, \lambda_2, \ldots, \lambda_{n-2}, a + bi, a - bi,$$

where eigenvalues λ_1 through λ_{n-2} have negative real parts and λ_{n-1}, λ_n (precisely these two) are complex conjugates that cross the imaginary axis when γ varies through some critical value, then the theorem still predicts closed (limit-cycle) trajectories. The extension of this theorem to arbitrary dimensions depends in large part on another important theorem (called the *center manifold theorem*), which ensures that close to the steady state the interesting events take place on a plane-like subset of R^n (mathematically called a *two-dimensional manifold*).

curves represent stable steady states or periodic solutions, whereas dotted curves represent unstable states.)

While in Figure 8.19(a,b) the limit cycle is shown originating at γ^*, the theorem actually does not specify at what exact value the closed orbit appears. Furthermore, to determine whether or not the limit cycle is stable a rather complicated calculation must be done. A simple case is given as an example in the following box. Other examples can be found in Marsden and McCracken (1976, sections 4a,b), Odell (1980), Guckenheimer and Holmes (1983) and Rand et al. (1981).

Calculations of Stability of the Limit Cycle in Hopf Bifurcation for the Case $n = 2$

For the system of equations (33a,b) it will be assumed that for $\gamma = \gamma^*$ the Jacobian matrix is of the form

$$\mathbf{J} = (\bar{x}, \bar{y})\,|_{\gamma=\gamma^*} = \begin{pmatrix} 0 & 1 \\ -b & 0 \end{pmatrix}. \tag{35}$$

In this case the eigenvalues (at the critical parameter value) are

$$\lambda_1 = bi, \qquad \lambda_2 = -bi.$$

Marsden and McCracken (1976) derive a rather elaborate stability criterion.

The following expression must be calculated and evaluated at the steady state when $\gamma = \gamma^*$:

$$V''' = \frac{3\pi}{4b}(f_{xxx} + f_{xyy} + g_{xxy} + g_{yyy}) + \frac{3\pi}{4b^2}[f_{xy}(f_{xx} + f_{yy}) + g_{xy}(g_{xx} + g_{yy}) + f_{xx}g_{xx} - f_{yy}g_{yy}]. \tag{36}$$

Then the conclusions are as follows:

1. If $V''' < 0$, then the limit cycle occurs for $\gamma > \gamma^*$ (supercritical) and is stable.
2. If $V''' > 0$, the limit cycle occurs for $\gamma < \gamma^*$ (subcritical) and is repelling (unstable).
3. If $V''' = 0$, the test is inconclusive.

Note: If the Jacobian matrix obtained by linearization of equations (33a,b) has diagonal terms but the eigenvalues are still complex and on the imaginary axis when $\gamma = \gamma^*$, then it is necessary to *transform variables* so that the Jacobian appears as in (35) before the stability receipe can be applied. (See Marsden and McCracken, 1976, for several examples.)

Example 1

Consider the system of equations

$$\frac{dx}{dt} = y = f(x, y; \gamma), \tag{37a}$$

$$\frac{dy}{dt} = -y^3 + \gamma y - x = g(x, y; \gamma). \tag{37b}$$

(This system comes from Marsden and McCracken, 1976, pp. 136, and references therein.) We consider these equations, where γ plays the role of a bifurcation parameter.

The only steady state occurs when $x = y = 0$; at that point the Jacobian is

$$\mathbf{J}(0, 0) = \begin{pmatrix} f_x & f_y \\ g_x & g_y \end{pmatrix} = \begin{pmatrix} 0 & 1 \\ -1 & \frac{-y^2}{3} + \gamma \end{pmatrix}_{(0,0)} = \begin{pmatrix} 0 & 1 \\ -1 & \gamma \end{pmatrix} \tag{38}$$

Eigenvalues of this system are given by

$$\lambda = \frac{\gamma \pm \sqrt{\gamma^2 - 4}}{2}. \tag{39}$$

In the range $|\gamma| < 2$, the eigenvalues are complex $\lambda = \{a \pm bi\}$, where

$$a = \operatorname{Re} \lambda = \frac{\gamma}{2} \quad \text{and} \quad b = \operatorname{Im} \lambda = \frac{(\sqrt{4 - \gamma^2})}{2}.$$

Note that as γ increases from negative values through 0 to positive values, the eigen-

values cross the imaginary axis. In particular, at the bifurcation value $\gamma = 0$ we have

$$\lambda = \pm i$$

(pure imaginary eigenvalues) and $da/d\gamma \neq 0$.

The Hopf bifurcation theorem therefore applies, predicting the existence of periodic orbits for equations (37a,b). We next calculate the expression V''' and determine stability. For equations (37a,b) we have

$$\begin{aligned} f_{xxx} &= 0, & f_{xy} &= 0, \\ f_{xyy} &= 0, & g_{xy} &= 0, \\ g_{xxy} &= 0, & f_{xx} &= 0, \\ g_{yyy} &= -6, & f_{yy} &= 0. \end{aligned} \tag{40}$$

This means that

$$\begin{aligned} V''' &= \frac{3\pi}{4b}(0 + 0 + 0 - 6) + \frac{3\pi}{4b^2}(0) \\ &= \frac{3\pi}{4}(-6) < 0. \end{aligned} \tag{41}$$

This falls into case 1 (see previous box), and so the limit cycle is stable.

8.7 OSCILLATIONS IN POPULATION-BASED MODELS

A number of natural populations are known to exhibit long-term oscillations. Although conjectures about the underlying mechanisms vary, it is commonly recognized that the relationship between prey and predators can lead to such fluctuations in species abundance.

One model that predicts the tendency of predator-prey systems to oscillate is the Lotka-Volterra model, which we discussed in some detail in Chapter 6, Section 6.2. As previously remarked, however, this model is not sufficiently faithful to the real dynamical behavior of populations. Part of the problem stems from the fact that the Lotka-Volterra model is structurally unstable, that is, subject to drastic changes when relatively minor changes are made in the equations. A second problem is that the cycles in species abundance are sensitive to initial population levels. For example, if we start with large populations, the fluctuations too will be very large (see Figure 6.4a). (In the next section we shall discover that this property stems from the fact that the Lotka-Volterra system is *conservative*.)

Since oscillations in natural populations are more regular and stable than those of the simple Lotka-Volterra model, we explore the possibility that the underlying dynamical behavior suitable for depicting these is the limit cycle. Our main goal in this section is to start with a more general set of equations, retain some of the properties of the predator-prey model, and make minimal further assumptions in order to ensure that stable limit-cycle oscillations exist. (This approach is to some extent similar to problems discussed in Sections 3.5, 4.11, and 7.7.) With the theory of Poincaré, Bendixson, and Hopf, we are in a position to reason geometrically and analytically about stable oscillations.

As a starting set of equations we shall consider

$$\frac{dx}{dt} = xf(x, y), \tag{42a}$$

$$\frac{dy}{dt} = yg(x, y), \tag{42b}$$

where x is the prey density, y is the predator density, and the functions f and g represent the species-dependent per capita growth and death rates. Furthermore, we consider, as before, spatially uniform populations comprised of identical individuals.

Based on this form we may conclude that system (42) has nullclines that satisfy

$$\dot{x} = 0: \quad x = 0 \quad \text{or} \quad f(x, y) = 0, \tag{43a}$$

$$\dot{y} = 0: \quad y = 0 \quad \text{or} \quad g(x, y) = 0. \tag{43b}$$

Thus the x and y axes are nullclines, as are the other loci described by equations (43a,b). We shall assume that the loci corresponding to $f(x, y) = 0$ and $g(x, y) = 0$ are single curves and that these intersect once in the positive xy quadrant at $(\bar{x}, \bar{y})$; that is, that there is a single, strictly positive steady state.

In connection with these assumptions, recall that in the Lotka-Volterra model, $f(x, y) = 0$, $g(x, y) = 0$ are straight lines, parallel to the x or y axes respectively, and that the steady state at their intersection is a neutral center for all parameter values. This presents two features to be corrected if we are to discover stable limit-cycle solutions. First, as evident from Figure 6.4, there is the possibility of flow escaping to infinitely large x values, whereas, to use the Poincaré-Bendixson theorem we are required to exhibit a *bounded* region that traps flow. Second, if we were to exploit the Hopf bifurcation theorem, the steady state should not be forever poised at the brink of neutral stability; rather, it should undergo some transition (from stable to unstable focus) as parameters are changed.

We now list four assumptions that will be made in view of the minimal information consistent with the biological system.

1. $\partial f/\partial y < 0$ (Predators adversely affect the prey; that is, net growth rate of the prey population is smaller when they are being exploited by more predators.)
2. $\partial g/\partial x > 0$ (The availability of more prey enhances the predator's growth rate.)
3. There is a threshold level of predators, y_1, that reduces the per capita prey growth rate to zero (even when the prey population is very small); that is, y_1 is defined by
$$f(0, y_1) = 0.$$
4. There is a level of prey x_1 that is minimally required to sustain the predator population; x_1 is defined by the relationship
$$g(x_1, 0) = 0.$$

Assumptions 3 and 4 simply mean that we retain the property that prey (x) and

predator (y) nullclines intersect the predator and prey axes as in Figure 8.20(a). Further, assumptions 1 and 2 imply that along the y and x axes the flow is respectively toward and away from (0, 0) (see problem 17). Moreover, this also determines the directions of flow along the nullclines $f(x, y) = 0$ and $g(x, y) = 0$ since continuity must be preserved.

We now consider what other minimal assumptions could produce a geometrical situation to which the Poincaré-Bendixson theorem might apply, that is, a region in the xy plane that confines flow. According to our previous remark, it is necessary to prevent the escape of trajectories along the x axis to infinite x values. This could be

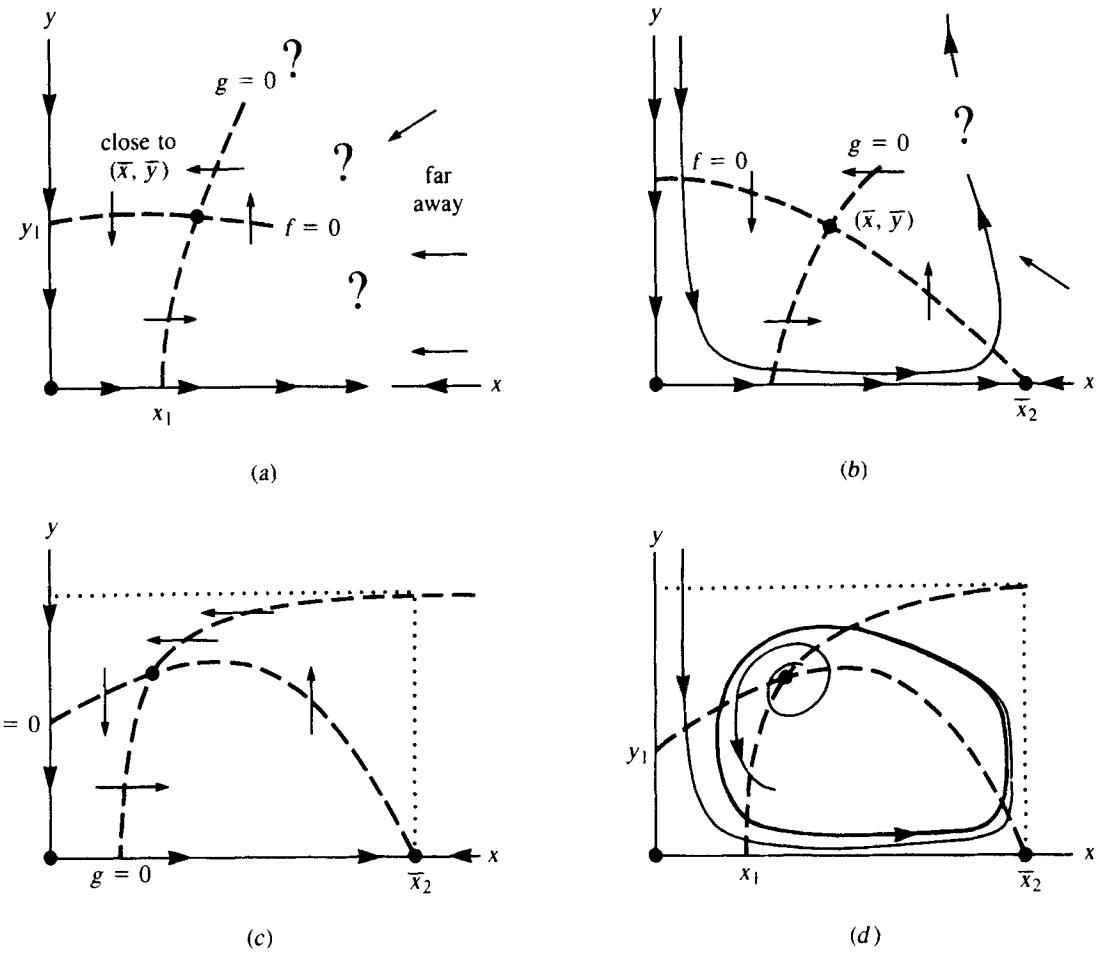

Figure 8.20 *The Lotka-Volterra model of Section 6.2 must be changed to ensure that a trajectory-trapping region surrounds* $(\bar{x}, \bar{y})$. *(a) Far away flow must be towards decreasing* x *and* y *values. (b) Flow along the* x *direction can be reversed by allowing for a steady state at* $(\bar{x}_2, 0)$, *in absence of predators. (c) Flow along the* y *axis can be controlled by bending the* y *nullcline* (g = 0). *To ensure that* $(\bar{x}, \bar{y})$ *is unstable, the curve* f = 0 *must have positive slope at its intersection with* g = 0 *(hence* f = 0 *has a "hump"). These conditions lead to a stable limit cycle, shown in (d).*

done by assuming that there is a second steady state somewhere along the positive x axis, at $(\bar{x}_2, 0)$. At such a point the flow will be halted and reversed. The appropriate assumption is that

5. There is a value of x, say $\bar{x}_2$, such that $(\bar{x}_2, 0)$ is also a steady state.

In other words, in the absence of predators, the prey population will eventually attain a constant level given by its natural carrying capacity, here denoted as $\bar{x}_2$. The prey population does not continue to grow ad infinitum.

An easy way of achieving this predation-free steady state geometrically is to bend the curve $f(x, y) = 0$ so that it intersects the x axis at $\bar{x}_2$, in other words, so that $f(\bar{x}_2, 0) = 0$ is exactly as shown in Figure 8.20(b). This then implies that

6. The x-nullcline corresponding to $f(x, y) = 0$ has *a negative slope* for prey levels that are sufficiently large (so that it eventually comes down and intersects the x axis).

The condition can be made precise by implicit differentiation: Everywhere on the curve

$$f(x, y) = 0 \tag{44}$$

it is true that

$$\frac{\partial f}{\partial x}\frac{dx}{dx} + \frac{\partial f}{\partial x}\frac{dy}{dx} = 0, \tag{45}$$

that is,

$$\frac{\partial f}{\partial x} + \frac{\partial f}{\partial y}s = 0, \tag{46}$$

where $s = dy/dx$ is the slope of the curve. Requiring a negative slope means that

$$s = -\frac{\partial f/\partial x}{\partial x/\partial y} < 0 \qquad \text{(for large } x\text{)}.$$

By assumption 1 this can only be true if

$$\frac{\partial f}{\partial x} < 0 \qquad \text{(for large } x\text{)}. \tag{47}$$

This means that at large population levels the prey's growth rate diminishes as density increases. The qualifier "large x" simply means that we wish the intersection $\bar{x}_2$ to occur at prey values bigger that x_1 (see problem 17).

The above six conditions lead to the sketch shown in Figure 8.20(b). This restricts flow along the x axis but is not sufficient to rule out narrow but infinitely long flow regimes down the y axis, around the steady state, and back up to $y \to \infty$. The problem is alleviated by suitably positioning the "tail end" of the y nullcline $g(x, y) = 0$. Figure 8.20(c) illustrates the way to proceed. We see that the slope of

this curve is positive for all values of x. By implicit differentiation it can be established (as previously) that this leads to a condition on g, namely

7. $$\partial g/\partial y < 0. \tag{48}$$

We see that the predator population also experiences density-dependent growth regulation and cannot grow explosively, even in an abundance of prey.

Conditions 1 to 7 result in the phase-plane behavior shown in Figure 8.20(c). To summarize, we have now obtained a subset of the xy plane, shown as a dotted rectangle in Figure 8.20(c) from which flow cannot depart. In order to obtain a limit cycle it is now necessary to ensure that the steady state $(\bar{x}, \bar{y})$ is unstable (repellent) so that the conditions of the Poincaré-Bendixson theorem will be met. To determine the constraints that this requirement imposes, we define the Jacobian of equations (42):

$$\mathbf{J} = \begin{pmatrix} \dfrac{\partial(xf)}{\partial x} & \dfrac{\partial(xf)}{\partial y} \\ \dfrac{\partial(yg)}{\partial x} & \dfrac{\partial(yg)}{\partial y} \end{pmatrix}_{(\bar{x}, \bar{y})} \equiv \begin{pmatrix} a & b \\ c & d \end{pmatrix}. \tag{49}$$

Then, since $f(\bar{x}, \bar{y}) = g(\bar{x}, \bar{y}) = 0$, we have

$$a = xf_x|_{ss}, \tag{50a}$$
$$b = xf_y|_{ss}, \tag{50b}$$
$$c = yg_x|_{ss}, \tag{50c}$$
$$d = yg_y|_{ss}. \tag{50d}$$

[where ss denotes that the quantities are to be evaluated at $(\bar{x}, \bar{y})$]. Furthermore, requiring $(\bar{x}, \bar{y})$ to be an unstable node or focus is equivalent to the conditions for two positive eigenvalues of (49):

$$a + d > 0, \tag{51a}$$
$$ad - bc > 0. \tag{51b}$$

Details leading to this result and further comments are given in problem 18. It transpires that the appropriate instability at $(\bar{x}, \bar{y})$ can only be obtained if one assumes that at $(\bar{x}, \bar{y})$ the slope of the nullcline $f(x, y) = 0$ is positive but smaller than that of the nullcline $g(x, y) = 0$; that is,

$$0 < s_f(\bar{x}, \bar{y}) < s_g(\bar{x}, \bar{y}). \tag{52}$$

where

$$s_f(x, y) = \left.\frac{dy}{dx}\right|_{(\bar{x}, \bar{y})}$$

is the slope of the nullcline $f(x, y) = 0$, and similarly s_g is the slope of $g(x, y) = 0$ at $(\bar{x}, \bar{y})$. Therefore, the curve $f(x, y) = 0$ must have curvature as shown in Figure 8.20(c), with $(\bar{x}, \bar{y})$ to the left of the hump.

With this informal reasoning we have essentially arrived at a rather famous theorem due to Kolmogorov, summarized here:

Kolmogorov's Theorem

For a predator-prey system given by equations (42a,b) let the functions f and g satisfy the following conditions:

1. $\partial f/\partial y < 0$;
2. $\partial g/\partial x > 0$;
3. For some $y_1 > 0, f(0, y_1) = 0$.
4. For some $x_1 > 0$, $g(x_1, 0) = 0$.
5. There exists $\bar{x}_2 > 0$ such that $f(\bar{x}_2, 0) = 0$.
6. $\partial f/\partial x < 0$ for large x (equivalently, $\bar{x}_2 > x_1$), but $\partial f/\partial x > 0$ for small x.
7. $\partial g/\partial y < 0$.
8. There is a positive steady state $(\bar{x}, \bar{y})$ that is unstable; that is
$$(xf_x + yg_y)_{ss} > 0 \qquad \text{and} \qquad (f_x g_y - f_y g_x)_{ss} > 0.$$
9. Moreover, $(\bar{x}, \bar{y})$ is located on the section of the curve $f(x, y) = 0$ whose slope is positive.

Then there is a (strictly positive) limit cycle, and the populations will undergo sustained periodic oscillations.

Figure 8.20(d) depicts the nature of these oscillations in the xy plane.

A Summary of the Biological Conditions Leading to Predator-Prey Oscillations

1. An increase in the predator population causes a net decrease in the per capita growth rate of the prey population.
2. An increase in the prey density results in an increase in the per capita growth rate of the predator population.
3. There is a predator density y_1 that will prevent a small prey population from growing.
4. There is a prey density x_1 that is minimally required to maintain growth in the predator population.

5, 6. Growth rate of the prey is density-dependent, so that there is a density $\bar{x}_2$ at which the trend reverses from net growth to net decline. At small densities an increase in the population leads to increased net rate of growth (for example, by enhancing reproduction or survivorship). The opposite is true for densities greater than $\bar{x}_2$. (This is the so-called Allee effect, discussed in Section 6.1.)

7. The predator population undergoes density-dependent growth. As density increases, competition for food or similar effects causes a net decline in the growth rate (for example, by decreasing the rate of reproduction).
8. The species coexistence at some constant levels $(\bar{x}, \bar{y})$ is unstable, so that small fluctuations lead to bigger fluctuations. This is what creates the limit-cycle oscillations.

These eight conditions are sufficient to guarantee stable population cycles in any system in which one of the species exploits the other (sometimes called an *exploiter-victim system;* see Odell, 1980, for example). Of course it should be remarked that other population interactions may also lead to stable oscillations and that we have by no means exhausted the list of reasonable interactions leading to the appropriate dynamics.

For an example of oscillations in a plant-herbivore system, see problem 21. You may wish to consult Freedman (1980) for more details and an extensive bibliography, or Coleman (1983) for a good summary of this material.

8.8 OSCILLATIONS IN CHEMICAL SYSTEMS

The discovery of oscillations in chemical reactions dates back to 1828, when A.T.H. Fechner first reported such behavior in an electrochemical cell. About seventy years later, in the late 1890s, J. Liesegang also discovered periodic precipitation patterns in space and time. The first theoretical analysis, dating back to 1910 was due to Lotka (whose models are also used in an ecological contex; see Chapter 6). However, misconceptions and old ideas were not easily changed. The scientific community held the unshakable notion that chemical reactions always proceed to an equilibrium state. The arguments used to support such intuition were based on thermodynamics of *closed* systems (those that do not exchange material or energy with their environment). It was only later recognized that many biological and chemical systems are *open* and thus not subject to the same thermodynamic principles.

Over the years other oscillating reactions have been found (see, for example, Bray, 1921). One of the most spectacular of these was discovered in 1959 by a Russian chemist, B. P. Belousov. He noticed that a chemical mixture containing citric acid, acid bromate, and a cerium ion catalyst (in the presence of a dye indicator) would undergo striking periodic changes in color, right in the reaction beaker. His results were greeted with some skepticism and disdain, although his reaction (later studied also by A. M. Zhabotinsky) has since received widespread acclaim and detailed theoretical treatment. It is now a common classroom demonstration of the effects of nonlinear interactions in chemistry. (See Winfree, 1980 for the recipe and Tyson, 1979, for a review.)

The bona fide acceptance of chemical oscillations is quite recent, in part owing to the discovery of oscillations in biochemical systems (for example, Ghosh and Chance, 1964; Pye and Chance, 1966). After much renewed interest since the early 1970s, the field has blossomed with the appearance of hundreds of empirical and theoretical publications. Good summaries and references can be found in Degn (1972), Nicolis and Portnow (1973), Berridge and Rapp (1979), and Rapp (1979).

The first theoretical work on the subject by Lotka (discussed presently) led to a reaction mechanism which, like the Lotka-Volterra model, suffered from the defect of structural instability. That is, his equations predict neutral cycles that are easily disrupted when minor changes are made in the dynamics. An important observation is that this property is shared by all *conservative systems* of which the Lotka system is an example. A simple mechanical example of a conservative system is the ideal linear pendulum: the amplitude of oscillation depends only on its initial configura-

tion since some quantity (namely the total energy in this mechanical system) is conserved. Such systems cannot lead to the structurally stable limit-cycle oscillations. It can be shown (see box) that in the Lotka system there is a quantity that remains constant along solution curves. Each value of this constant corresponds to a distinct periodic solution. (Thus there are uncountably many closed orbits, each within an infinitesimal distance of one another.) This leads to structural instability.

Lotka's Reaction

The following mechanism was studied by Lotka (1920):

$$\begin{aligned} A + x_1 &\xrightarrow{k_1} 2x_1, \\ x_1 + x_2 &\xrightarrow{k_2} 2x_2, \\ x_2 &\xrightarrow{k_3} B. \end{aligned} \tag{53}$$

Corresponding equations are

$$\frac{dx_1}{dt} = -kAx_1 + 2k_1Ax_1 - k_2x_1x_2 = k_1Ax_1 - k_2x_1x_2 \tag{54a}$$

$$\frac{dx_2}{dt} = -k_2x_1x_2 + 2k_2x_1x_2 - k_3x_2 = k_2x_1x_2 - k_3x_2 \tag{54b}$$

When the substance A is maintained at a constant concentration, the above equations (after renaming constants) are identical with the predator-prey model analyzed in some detail in Chapter 6. The presence of a steady state with neutral cycles is thus clear.

It can also be shown that the following expression is constant along trajectories:

$$v = x_1 + x_2 - \frac{k_3}{k_2}\ln x_1 - \frac{k_1A}{k_2}\ln x_2. \tag{55}$$

To see this it is necessary to rewrite the system of equations (54) as follows:

$$\frac{dx_1}{dx_2} = \frac{k_1Ax_1 - k_2x_1x_2}{k_2x_1x_2 - k_3x_2}, \tag{56}$$

or equivalently as

$$\left(1 - \frac{k_3}{k_2x_1}\right)dx_1 + \left(1 - \frac{k_1A}{k_2x_2}\right)dx_2 = 0. \tag{57}$$

Now we shall discuss the properties of this so called *exact* equation.

Let us inquire whether the LHS of equation (57) can be written as a total differential of some scalar function $v(x_1, x_2)$. If so then

$$dv = 0, \tag{58}$$

(which means that v is a constant). This implies that

$$\frac{\partial v}{\partial x_1}dx_1 + \frac{\partial v}{\partial x_2}dx_2 = 0. \tag{59}$$

Let us define the following, taken from expressions in equation (57):

$$M = 1 - \frac{k_3}{k_2 x_1}, 1 \qquad N = 1 - \frac{k_1 A}{k_2 x_2}. \tag{60}$$

These should satisfy the relations

$$Mdx_1 + Ndx_2 = 0$$

where

$$M = \frac{\partial v}{\partial x_1}, \qquad N = \frac{\partial v}{\partial x_2}. \tag{61}$$

As will be emphasized in Chapter 10 in connection with partial differentiation, this can only be true when the following relation between M and N holds (provided v has continuous second partial derivatives):

$$\frac{\partial M}{\partial x_2} = \frac{\partial v}{\partial x_2 \partial x_1} = \frac{\partial v}{\partial x_1 \partial x_2} = \frac{\partial N}{\partial x_1}. \tag{62}$$

Checking equations (60) for this condition leads to

$$\frac{\partial M}{\partial x_2} = \frac{\partial}{\partial x_2}\left(1 - \frac{k_3}{k_3 x_1}\right) = 0 = \frac{\partial}{\partial x_1}\left(1 - \frac{k_1 A}{k_2 x_2}\right) = \frac{\partial N}{\partial x_1}. \tag{63}$$

Equations that satisfy (61), (62) are called *exact* equations. Once identified as such, they can be solved in a standard way (see problem 23). Geometrically the solution curves of such equations can be viewed as the *level curves* of a potential function (v in this case) or, in a more informal description, as the constant-altitude contours on a topographical map of a mountain range. (See Figure 8.21.) Each curve corresponds to a fixed "total energy", a fixed potential v, or a fixed height on the mountain, depending on the way one interprets the conserved quantity. Since there is an infinity of possible closed curves, they are neutrally but not asymptotically stable.

Just as it was possible to modify the Lotka-Volterra model in population dynamics, so too we can write modified Lotka reactions in which limit-cycle trajectories exist. (See problem 22.) This has been the basis of much recent work in the topic of oscillating reactions.

More generally, a number of guidelines and requirements for chemical oscillations has been established. A partial list follows.

Criteria for Oscillations in a Chemical System

1. The theory of Poincaré and Bendixson (in two dimensions) and Hopf bifurcations (in n dimensions) applies as before to a given system.
2. Some sort of feedback is required to obtain oscillations; following are

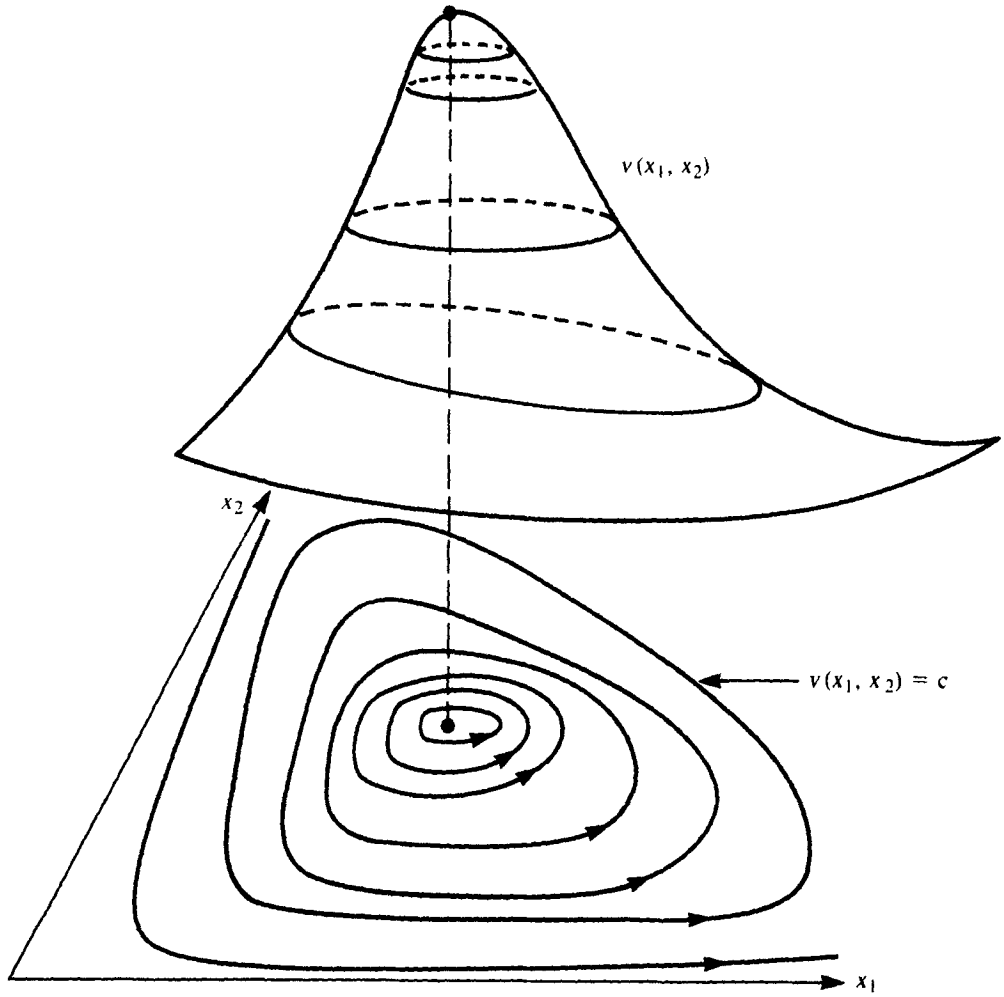

Figure 8.21 *A conservative system is characterized by the property that some quantity (for example, potential, total energy, or height on a hill) is constant along solution curves. Such systems can have neutrally stable cycles but* not *limit-cycle trajectories.*

examples of *activation* and *inhibition,* which are particular types of feedback:

activation

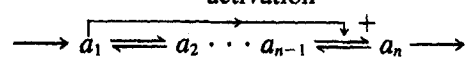

activation

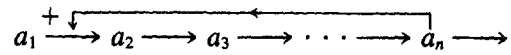

inhibition

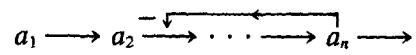

inhibition

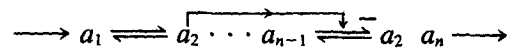

In these examples one of the chemicals affects the rate of a reaction step in the network. (Activation implies enhancing a reaction rate, whereas inhibition implies the opposite effect.) Since most biological reactions are mediated by enzymes, a common mechanism through which such effects could occur is *allosteric modification;* for example, the substrate attaches to the enzyme, thereby causing a conformational change that reduces the activity of the enzyme. It is common to refer to a *feedback* influence if the chemical has an effect on its *precursors* (substances required for its own formation). Similarly, *feedforward* refers to a chemical's influence on its *products* (those chemicals for which it is a precursor).

Nicolis and Portnow (1973) comment particularly on chemical systems that can be described by a pair of differential equations such as

$$\frac{dx_1}{dt} = v_1(x_1, x_2), \tag{64a}$$

$$\frac{dx_2}{dt} = v_2(x_1, x_2), \tag{64b}$$

The Lotka chemical system and equations (54a,b) would be an example of this type. Equations (64a,b) indicate that to obtain limit-cycle oscillations, one of the following two situations should hold:

2a. At least one intermediate, x_1 or x_2 is *autocatalytic,* (catalyses its own production or activates a substance that produces it).

2b. One substance participates in *cross catalysis* (x_1 activates x_2 or vice versa).

These two conditions are based on the mathematical prerequisites of the Poincaré-Bendixson theory (see Nicolis and Portnow, 1973). For more than two variables it has been shown the inhibition without additional catalysis can lead to oscillations.)

3. Thermodynamic considerations dictate that *closed chemical systems* (which receive no input and cannot exchange material or heat with their environment) cannot undergo sustained oscillations because as reactants are used up the system settles into a steady state.

4. Oscillations cannot occur close to a thermodynamic equilibrium (see Nicolis and Portnow, 1973, for definition and discussion).

Schnakenberg (1979), who also considers in generality the case of chemical reactions involving *two* chemicals, concludes that when each reaction has a rate that depends monotonically on the concentrations (meaning that increasing x_1 will always increase the rate of reactions in which it participates) trajectories in the x_1x_2 phase space are bounded. Thus, when the steady state of the network is an unstable focus, conditions for limit-cycle oscillations are produced.

The following additional observations were made by Schnakenberg:

1. Chemical systems with two variables and less than three reactions cannot have limit cycles.

2. Limit cycles can only occur if one of the three reactions is autocatalytic.
3. Furthermore, in such systems limit cycles will only occur if the autocatalytic step involves the reaction of at least three molecules. When exactly three molecules are involved, the reaction is said to be *trimolecular;* for example, the reaction (65a).

Details and further references may be found in Schnakenberg (1979).

To demonstrate oscillations in a simple chemical network, we consider a system described by Schnakenberg (1979):

$$2X + Y \rightleftharpoons 3X, \tag{65a}$$

$$\mathrm{A} \longrightarrow Y, \tag{65b}$$

$$X \longrightarrow \mathrm{B}. \tag{65c}$$

The network bears similarity to the Brusselator (see problem 20 of Chapter 7). It is also related to a model for the glycolytic oscillator due to Sel'kov (1968). The reaction is said to be trimolecular since there is a reaction step in which an encounter between three molecules is required. Presently we shall use this example for the purposes of illustrating techniques rather than as a prototype of real chemical oscillators, which tend to be far more complicated.

Before beginning the calculations, it is worth remarking that the network has an autocatalytic step (X makes more X), consists of three reaction steps, and has a trimolecular step. It is thus a prime candidate for oscillations.

Equations for the Schnakenberg system (65a,b,c) are as follows:

$$\frac{dx}{dt} = x^2y - x, \tag{66a}$$

$$\frac{dy}{dt} = a - x^2y, \tag{66b}$$

where x, y, and a are the concentrations of X, Y, and A. These have a steady state at $(\bar{x}, \bar{y}) = (a, 1/a)$ and a Jacobian

$$\mathbf{J} = \begin{pmatrix} 2xy - 1 & x^2 \\ -2xy & -x^2 \end{pmatrix}_{ss} = \begin{pmatrix} 1 & a^2 \\ -2 & -a^2 \end{pmatrix}; \tag{67}$$

since

$$\beta = \operatorname{Tr} \mathbf{J} = 1 - a^2, \tag{68a}$$

$$\gamma = \det \mathbf{J} = a^2(-1 + 2) = a^2, \tag{68b}$$

we observe that eigenvalues are

$$\lambda_{1,2} = \frac{(1 - a^2) \pm \sqrt{(1 - a^2)^2 - 4a}}{2}. \tag{69}$$

If $a^2 = 1$, these are pure imaginary ($\lambda = \pm ai$), and for $a^2 < 1$ eigenvalues have a positive real part, so that the steady state is an unstable focus. The Hopf bifurcation indicates the presence of a small-amplitude limit cycle as a is decreased from $a > 1$ to $a < 1$. However, the stability of the limit cycle is uncertain. Notice

that for $a = 1$ the Jacobian is not in the "normal" form necessary for direct determination of the stability expression V''' discussed in Section 8.6. While it is possible to transform variables to get this normal form, the calculations are formidably messy (and preferably avoided).

Looking at a phase-plane diagram of equations (66a,b) in Figure 8.22(a) reveals a problem: There is the possibility that close to the y axis trajectories may sweep off to $y = \infty$ so that it is impossible to define a Poincaré-Bendixson region that traps flow.

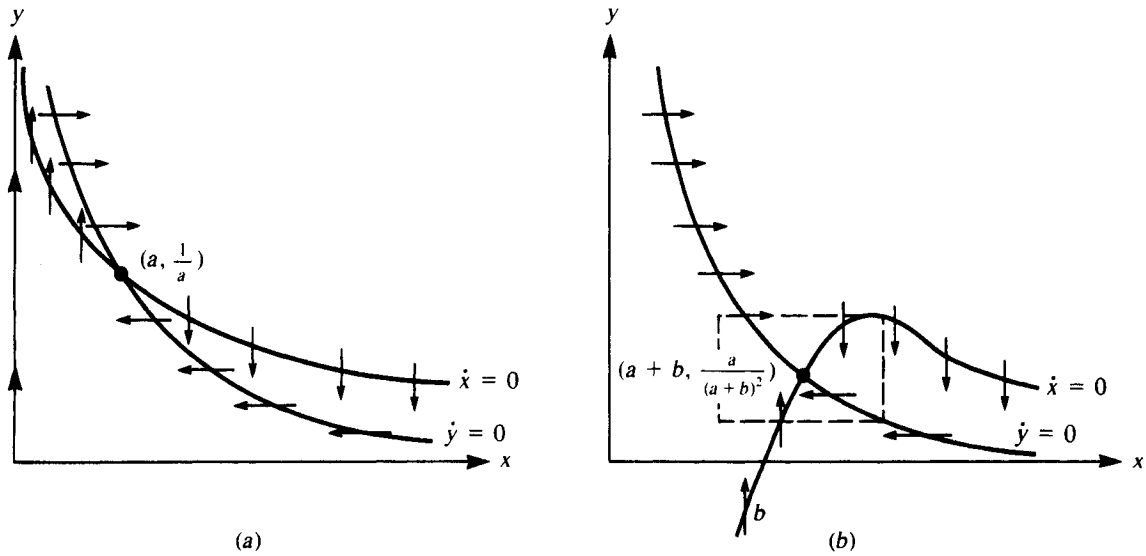

Figure 8.22 *(a) A simple chemical network taken from equations (66a,b) (suggested by Schnakenberg, 1979) has this qualitative phase plane. (b) (By modifying the system slightly to equations (70a,b), we can use the Poincaré-Bendixson theorem to conclude that a limit cycle exists somewhere in the dotted box.*

To circumvent this problem, Schnakenberg changed the last reaction step to a reversible one,

$$x \rightleftharpoons \mathrm{B}. \qquad (65c')$$

This changes the equations into the system

$$\frac{dx}{dt} = x^2y - x + b, \qquad (70a)$$

$$\frac{dy}{dt} = -x^2y + a. \qquad (70b)$$

The new steady state is $(a + b, a/(a + b)^2)$, and the new Jacobian is

$$\mathbf{J} = \begin{pmatrix} \dfrac{a-b}{a+b} & (a+b)^2 \\ \dfrac{-2a}{a+b} & -(a+b)^2 \end{pmatrix}. \tag{71}$$

Letting

$$\beta = \operatorname{Tr} \mathbf{J} = \frac{a-b}{a+b} - (a+b)^2, \tag{72a}$$

$$\gamma = \det \mathbf{J} = -(a-b)(a+b) + 2a(a+b) = (a+b)^2, \tag{72b}$$

we see that γ is always a positive quantity and that a bifurcation occurs when $\beta = 0$, that is, when

$$\frac{a-b}{a+b} = (a+b)^2. \tag{73}$$

The eigenvalues are then

$$\lambda_{1,2} = \frac{\pm\sqrt{-4\gamma}}{2} = \pm(a+b)i. \tag{74}$$

Suppose b is much smaller than a. An approximate result is that

$$\frac{a-b}{a+b} \simeq \frac{a}{a} = 1, \qquad (a+b)^2 \simeq a^2, \tag{75}$$

so that from equation (73) we have

$$a^2 \simeq 1.$$

Thus the bifurcation occurs close to $a = 1$. (For larger a values, the steady state is stable; for smaller values it is an unstable focus.) Again, the Hopf bifurcation theorem can be applied to conclude that closed periodic trajectories will be found.

Summary of Biological Factors Necessary for Limit-Cycle Dynamics

1. *Structural stability:* infinitesimal changes in parameters or terms appearing in the model description of the system should not totally disrupt the dynamic behavior (as in the Lotka-Volterra model).
2. *Open systems:* systems should be open in the thermodynamic sense. Systems that are not open have finite, nonrenewable components that are consumed. Such *closed* systems will eventually be dissipated and thus cannot undergo undamped oscillations.
3. *Feedback:* some form of autocatalysis or feedback is generally required to maintain oscillations. For example, a species may indirectly influence its growth rate by affecting a secondary species upon which it depends.
4. *Steady state:* the system must have at least one steady state. In the case of populations or chemical concentrations, this steady state must be strictly positive. For oscillations to occur, the steady state must be unstable.

5. *Limited growth:* there should be limitations on the growth rates of all intermediates in the system to ensure that *bounded* oscillations can occur.

(See Murray, 1977 for detailed discussion.)

Summary of Mathematical Criteria for the Existence of Limit Cycles

1. There must exist at least one steady state that loses stability to become an unstable node or focus. (See Appendix 1 to this chapter on *topological index theory*.)
2. At such a steady state, there must be complex eigenvalues $\lambda = a \pm bi$ whose real part a changes sign as some parameter in the equations is tuned (Hopf bifurcation).
3. A bounded annular region in xy phase space admits flow inwards but not outwards (Poincaré-Bendixson theory).
4. A region in the xy phase space must have the quantity $\partial F/\partial x + \partial G/\partial y$ change sign (Bendixson's negative criterion). This is a necessary but not a sufficient condition.
5. A region in the xy phase space must have the quantity $\partial(BF)/\partial x + \partial(BG)/\partial y$ change sign where B is any continuously differentiable function (Dulac's criterion). This is a necessary but not a sufficient condition.
6. One or more S-shaped nullclines, suitably positioned, often lead to oscillations or excitability. Examples are the Lienard equation or van der Pol oscillator.

(For more advanced methods see also Cronin, 1977.)

Now examining the phase-plane behavior of the modified system, we remark that the nullclines, given by curves

$$y = \frac{x - b}{x^2} \qquad \left(\frac{dx}{dt} = 0\right), \tag{76a}$$

$$y = \frac{a}{x^2} \qquad \left(\frac{dy}{dt} = 0\right), \tag{76b}$$

prevent flow from leaving a finite region in the first quadrant. Thus, by the Poincaré-Bendixson theory, it can be conclusively established that stable periodic behavior results whenever the steady state is unstable.

8.9 FOR FURTHER STUDY: PHYSIOLOGICAL AND CIRCADIAN RHYTHMS

One of the earliest recorded observations of biological rhythms was made by an officer in the army of Alexander the Great who noted (in 350 BC) that the leaves of certain plants were open during daytime and closed at night. Until the 1700s such rhythms were viewed as passive responses to a periodic environment, that is, to the succession of light and dark cycles due to the natural day length (see Figure 8.23).

Figure 8.23 *In 1751 Linnaeus designed a "flower clock" based on the times at which petals for various plant species opened and closed. Thus, a botanist should be able to estimate the time of day without a watch merely by noticing which flowers were open. [Drawing by Ursula Schleicher-Benz from* Lindauer Bilderbogen *no. 5, edited by Friedrich Boer. Copyright by Jan Thorbecke Verlag, eds., Sigmaringen, West Germany.]*

In 1729 the astronomer Jean Jacques d'Ortous De Mairan conducted experiments with a plant and reported that its periodic behavior persisted in a total absence of light cues. Although his results were disputed at first, further demonstrations and experiments by others (such as Wilhelm Pfeffer, in 1875, 1915) gave clear evidence in

support of the observations that many physiological rhythms are *endogeneous* (independent of any external environment influences).

We now know that most organisms have innate "clocks" that govern peaks of activity, times devoted to sleep, and a variety of physiological states that fluctuate over the course of time. Rhythms close in period to the day length have been called *circadian*. Recent experimental work on a variety of organisms, including numerous plants, the fruitfly *Drosophila*, a variety of fungi, bees, birds, and mammals have been carried out (C. S. Pittendrigh, E. Bunning, J. Aschoff, R. A. Wever, A. T. Winfree). The results are often intriguing. For example, the circadian clocks of migratory birds allow them to navigate by compensating for the constantly shifting position of the sun.

As yet, our knowledge of the basic mechanisms underlying circadian rhythm, as well as other longer or shorter physiological cycles, remains uncertain. It appears that there are often numerous distinct physiological or cellular oscillators that are *coupled* (influence one another) but that maintain certain mutually independent characteristics. A brief summary of theoretical questions related to such problems is given by Winfree (1979). For fascinating historical summaries see Reinberg and Smolensky (1984) and Moore-Ede et al. (1982). Other references are provided as a starting point for further independent research on this topic. An excellent up-to-date synopsis of the human sleep-wake cycle is given by Strogatz (1986).

PROBLEMS*

1. Discuss what is meant by the statement that a limit cycle must be a *simple* closed curve. Why is Figure 8.1(*b*) not permissible? Why is Figure 8.1(*c*) not a limit cycle?

2. Consider the following system of equations (Lefschetz, 1977):

$$\frac{dx}{dt} = y = f(x, y),$$

$$\frac{dy}{dt} = x(a^2 - x^2) + by = g(x, y) \qquad (a \neq 0, b \neq 0).$$

(a) Show that the critical points are $(0, 0)$, $(a, 0)$, and $(-a, 0)$.
(b) Evaluate the expression $\partial f/\partial x + \partial g/\partial y$ at these steady states.
(c) Use Bendixson's negative criterion to rule out the presence of limit-cycle solutions about each one of these steady states.
(d) Sketch the phase-plane behavior.

***3.** Use Bendixson's negative criterion to show that if P is an isolated saddle point there cannot be a limit cycle in the neighborhood of P that contains only P.

4. Use Bendixson's negative criterion to indicate whether or not limit cycles can be ruled out in the following systems of equations in the indicated regions of the plane:

* Problems preceded by an asterisk (*) are especially challenging.

(a) $\dfrac{dx}{dt} = 2x - 3y,$
$\dfrac{dy}{dt} = 10x + y,$
(in R^2).

(b) $\dfrac{dx}{dt} = x + 2y(\sin^2 y) + y^{1/2},$
$\dfrac{dy}{dt} = xe^x + \dfrac{x^2}{2} + y,$
(in R^2).

(c) $\dfrac{dx}{dt} = a_1x + b_1y + c_1x^2,$
$\dfrac{dy}{dt} = d_2x + b_2y + c_2y^2,$
($x > 0, y > 0$).

(d) $\dfrac{dx}{dt} = ax - bxy,$
$\dfrac{dy}{dt} = -cy + dxy,$
($x > 0, y > 0$).

5. Show that Dulac's criterion but not Bendixson's criterion can be used to establish the fact that no limit cycles exist in the two-species competition model given in Section 6.3. (Hint: Let $B(x, y) = 1/xy$.)

6. Consider the following system of equations (Odell, 1980), which are said to describe a predator-prey system:

$$\frac{dx}{dt} = x[x(1 - x) - y],$$
$$\frac{dy}{dt} = k\left(x - \frac{1}{\mu}\right)y.$$

(a) Interpret the terms in these equations.

(b) Sketch the nullclines in the xy plane and determine whether the Poincaré-Bendixson theory can be applied.

(c) Show that the steady states are located at

$$(0, 0), \qquad (1, 0), \qquad \left(\frac{1}{\mu}, \frac{1 - 1/\mu}{\mu}\right).$$

(d) Show that at the last of these steady states the linearized system is characterized by the matrix

$$\begin{pmatrix} \dfrac{1}{\mu}\left(1 - \dfrac{2}{\mu}\right) & -\dfrac{1}{\mu} \\ \dfrac{k}{\mu}\left(1 - \dfrac{1}{\mu}\right) & 0 \end{pmatrix}$$

(e) Can the Bendixson negative criterion be used to rule out limit-cycle oscillations?

(f) If your results so far are not definitive, consider applying the Hopf bifurcation theorem. What is the stability of the strictly positive steady state? What is the bifurcation parameter, and at what value does the bifurcation occur?

***(g)** Show that at bifurcation the matrix in part (d) is not in the "normal" form required for Hopf stability calculations. Also show that if you transform the variables by defining

$$\tilde{x} = x, \qquad \tilde{y} = \frac{2}{k^{1/2}} y,$$

you obtain a new system that is in normal form.

***(h)** Find the transformed system, calculate V''' and show that it is negative.

(i) What conclusions can be drawn about the system?

7. If all steady states (indicated by large dots) in Figures (a) through (d) are unstable, can the Poincaré-Bendixson theorem be applied to prove existence of limit cycles?

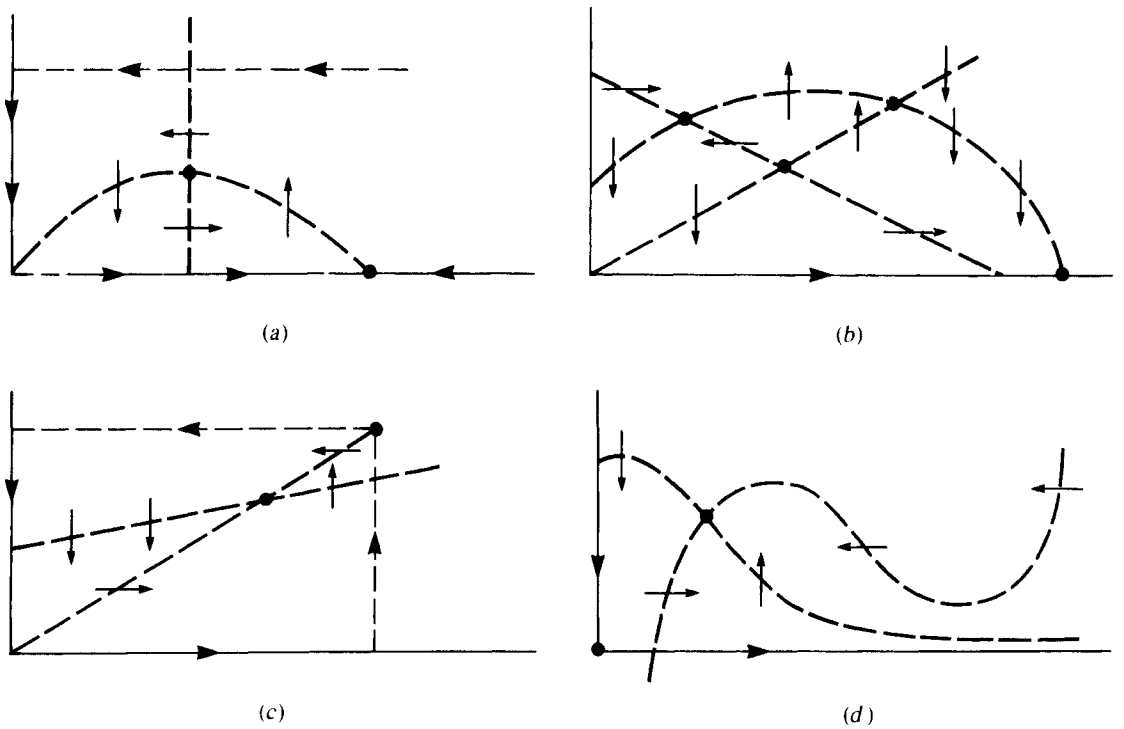

Figures for problem 7.

8. *The Hodgkin-Huxley model*

(a) What might be an interpretation of equations (10) and (11)? Of (12a–c)?

(b) Sketch the functions given in equations (13a–c). You may do this by hand or by computer.

(c) Discuss Fitzhugh's assumption that V and m change more rapidly than h and n.

(d) Demonstrate that the nullclines of Fitzhugh's reduced system are as shown in Figure 8.10(*a*).

9. *The Fitzhugh model*

(a) Verify the Jacobian given by (28) and the stability conditions of equations (30a,b).

(b) Show that the steady state of Fitzhugh's model is stable if it falls in the range

$$-\gamma \leq \bar{x} \leq \gamma$$

provided $b < 1$, $b < c^2$ and $\gamma = (1 - b/c^2)^{1/2}$.

(c) Show that this constraint places $\bar{x}$ on the portion of the cubic nullcline between the two humps.

10. (a) Graph the functions $G_1(u) = u^3$ and $G_2(u) = u^3/3 + 1$. In what way do these differ from the function $v = G(u)$ shown in Figure 8.13(*a*)?

(b) Draw nullclines and sketch the phase-plane flow behavior for the system of equations (15) where $G = G_1(u)$ and $G = G_2(u)$ given in part (a).

11. (a) Show that the Lienard equation (19) is equivalent to the system of equations (15a,b) where $G(u)$ is given by equation (20).

(b) Give justification for the claim that condition 1 of Section 8.4 guarantees that all trajectories will be symmetric about the origin.

(c) Show that condition 3 implies that (0, 0) is an unstable steady state of (15) where $G(u)$ is given by equation (20).

(d) If $G(u)$ satisfies conditions 1 to 3 and $\alpha = \beta$, give a reason for the assertion that there can be only one limit cycle in the Lienard system.

***12. (a)** *The van der Pol oscillator.* Show that equations (15a,b) and (16) are equivalent to equation (21).

(b) Suppose ϵ in equations (22a,b) is a small quantity and that the solutions to (22) can be expressed as

$$u(t) = f_0(t) + \epsilon f_1(t) + \epsilon^2 f_2(t) + \cdots + \epsilon^n f_n(t) + \cdots$$
$$v(t) = g_0(t) + \epsilon g_1(t) + \epsilon^2 f_2(t) + \cdots + \epsilon^n g_n(t) + \cdots .$$

What equations do the functions f_0, g_0, f_1, g_1, f_2, and g_2 satisfy?

13. (a) Suggest a possible molecular mechanism that might lead to the equations derived by Murray (1981) and thus the nullcline formation shown in Figure 8.14. (*Hint:* refer to problem 22 of Chapter 7.)

(b) Of the various configurations in Figure 8.14, which would you expect to lead to a limit-cycle oscillation?

(c) Is it possible to determine the steady state and its stability directly from Murray's equations?

14. (a) Suggest a possible mechanism that would lead to the equations given by Fairen and Velarde (1979) for bacterial respiration (see Figure 8.15).

(b) How does this model compare with that of Murray?

15. (a) Demonstrate that the Segel-Goldbeter model for oscillations in the cyclic AMP signaling system leads to the phase-plane configuration shown in Figure 8.16. What has been assumed to obtain the reduced $\gamma\alpha$ system?

(b) Investigate the mechanism underlying the assumption for Φ that supposedly depicts allosteric kinetics of adenylate cyclase. (You may wish to consult original papers by Segel and Goldbeter or Segel, 1984.)

16. Morris and Lecar (1981) describe a semiqualitative model for voltage oscillations in the giant muscle fiber of the barnacle. In this system the important ions are potassium and calcium (not sodium). The equations they suggest are the following:

$$I = C\frac{dv}{dt} + g_L(v - v_L) + g_{Ca}M(v - v_{Ca}) + g_K N(v - v_K),$$

$$\frac{dM}{dt} = \lambda_M(v)[M_\infty(v) - M],$$

$$\frac{dN}{dt} = \lambda_N(v)[N_\infty(v) - N],$$

where

v = voltage,

M = fraction of open Ca^{2+} channels,

N = fraction of open K^+ channels.

(a) Interpret these three equations. For reasons detailed in their papers Morris and Lecar define the functions M_∞, λ_M, N_∞, and λ_N as follows:

$$M_\infty(v) = \frac{1}{2}\left(1 + \tanh\frac{v - v_1}{v_2}\right), \qquad N_\infty(v) = \frac{1}{2}\left(1 + \tanh\frac{v - v_3}{v_4}\right),$$

$$\lambda_M(v) = \overline{\lambda}_M \cosh\frac{v - v_1}{2v_2}, \qquad \lambda_N(v) = \overline{\lambda}_N \cosh\frac{v - v_3}{2v_4}.$$

(b) Sketch or describe the voltage dependence of these functions.

Note: $\cosh x = \dfrac{e^x + e^{-x}}{2}$, $\quad \sinh x = \dfrac{e^x - e^{-x}}{2}$,

$$\tanh x = \frac{\sinh x}{\cosh x}.$$

(c) Morris and Lecar consider the reduced vN system to be an approximation to the whole model. What assumption underlies this approximation?

(d) Show that in the reduced vN system the variables are constrained to satisfy the following inequalities:

$$0 < N < 1,$$

$$\frac{g_L v_L + g_K v_K + I}{g_L + g_K} < v < \frac{g_L v_L + g_{Ca} v_{Ca} + I}{g_L + g_{Ca}}.$$

(You may need to use the fact that $0 < M < 1$.)

(e) Give support for the configuration of nullclines shown in Figure 8.17(a). Notice that there is an intersection within the region described by the inequalities in part (d) of this problem.

(f) Suppose you are told that at the steady state the linearized system has a pair of complex eigenvalues $\lambda = a + bi$ such that $a + bi$ behaves as in Figure 8.17(b) as the current I changes. Use your results from parts (a) to (e) to make a statement about the existence and stability of a limit-cycle solution.

(g) Interpret this in the biological context of electrical signal propagation in the barnacle giant muscle fiber.

(h) Compare the assumptions and results obtained from this model to the Hodgkin-Huxley and Fitzhugh models.

(This problem could be extended to an independent project with in-class discussion. See Morris and Lecar, 1981, for other details.)

17. *Limit cycles in predator-prey systems.* In this problem we investigate details that arise in Section 8.7.

(a) Justify the particular form of equations (42a,b) used in discussing a predator-prey system.

***(b)** Suppose the orientations of the nullclines is as shown in Figure 8.20(*a*). Use conditions 1 and 2 in Section 8.7, along with the fact that *on* these curves $f(x, y) = 0$ and $g(x, y) = 0$ respectively, to reason that the direction of flow along nullclines must conform to that shown in Figure 8.20(*a*). (*Hint:* Use the inequalities to determine in which regions f, or g, must be positive and in which negative.)

(c) A condition for a limit cycle is that $\bar{x}_2 > x_1$. Interpret this biologically and describe why this inequality is necessary.

(d) Verify condition 7 [equation (48)] by implicit differentiation of $g(x, y) = 0$.

(e) A steady state $(\bar{x}, \bar{y})$ is unstable if any *one* of the eigenvalues of the equations [linearized about $(\bar{x}, \bar{y})$] has a positive real part. Why then is it necessary to have *two* positive eigenvalues to ensure that a limit cycle exists?

18. In this problem we compute the stability properties of the nonzero steady state of the predator-prey equations (42a,b).

(a) Find the Jacobian of equations (42a,b).

(b) Show that conditions for an unstable node or spiral at $(\bar{x}, \bar{y})$ are as given in equations (51a–b).

(c) Verify the following relationship between the slope s_g of the nullcline $g = 0$ and the partial derivatives of g:

$$\text{slope of } g \text{ nullcline:} \quad s_g = -\frac{g_x}{g_y}.$$

(d) Use the inequality $a + d > 0$ and the inequalities $f_y < 0$, $g_x > 0$, and $g_y < 0$ to establish the following result: for $(\bar{x}, \bar{y})$ to be an unstable node or spiral, it is necessary and sufficient that

$$\bar{x} f_x(\bar{x}, \bar{y}) > \bar{y} \left| g_y(\bar{x}, \bar{y}) \right|.$$

Why does this imply that

$$f_x(\bar{x}, \bar{y}) > 0?$$

Why does it follow that

$$s_f(\bar{x}, \bar{y}) > 0,$$

in other words, that the slope of the curve $f(x, y) = 0$ must be positive at the steady state?

(e) Use the inequality $ad - bc > 0$ to show that at the steady state

$$\bar{x}\bar{y}f_y g_x\left(\frac{s_f}{s_g} - 1\right) > 0.$$

Note: all quantities are evaluated at the steady state, as in part (i). Reason that this inequality implies that

$$s_f(\bar{x}, \bar{y}) < s_g(\bar{x}, \bar{y}).$$

19. The following predator-prey system is discussed by May (1974):

$$\frac{dH}{dt} = rH\left(1 - \frac{H}{K}\right) - \frac{kPH}{H + D} \qquad \text{(host)},$$

$$\frac{dP}{dt} = sP\left(1 - \frac{P}{\gamma H}\right) \qquad \text{(parasite)}.$$

(a) Interpret the terms appearing in these equations and suggest what the various parameters might represent.

(b) Sketch the H and P nullclines on an HP phase plane.

(c) Apply Bendixson's criterion and Dulac's criterion (for $B = 1/HP$).

20. A number of modifications of the Lotka-Volterra predator-prey model that have been suggested over the years are given in the last box in Section 6.2. By considering several combinations of prey density-dependent growth and predator density-dependent attack rate, determine whether such modifications might lead to limit-cycle oscillations. You may wish to do the following:

(a) Check to see whether the Kolmogorov conditions are satisfied.

(b) Plot nullclines by hand (or by writing a simple computer program and check to see whether the Poincaré-Bendixson conditions are satisfied.

(c) Determine the stability properties of steady states.

21. This problem arises in a model of a plant-herbivore system: (Edelstein-Keshet, 1986). Assume that a population of herbivores of density y causes changes in the vegetation on which it preys. An internal variable x reflects some physical or chemical property of the plants which undergo changes in response to herbivory. We refer to this attribute as the *plant quality* of the vegetation and assume that it may in turn affect the fitness or survivorship of the herbivores. If this happens in a graded, continuous interaction, plant quality may be modeled by a pair of ODEs such as

$$\frac{dx}{dt} = f(x, y) \qquad \text{(rate of change of vegetation quality)},$$

$$\frac{dy}{dt} = yg(x, y) \qquad \text{(herbivore density)}.$$

(a) In one case the function $f(x, y)$ is assumed to be

$$f(x, y) = x(1 - x)[\alpha(1 - y) + x] \qquad (0 \leq x \leq 1).$$

Sketch this as a function of x and reason that the plant quality x always remains within the interval $(0, 1)$ if $x(0)$ is in this range. Show that plant quality may either decrease or increase depending on (1) initial value of x

and (2) population of herbivores. For a given herbivore population density $\hat{y}$, what is the "breakeven" point (the level of x for which $dx/dt = 0$)?

(b) It is assumed that the herbivore population undergoes logistic growth (see Section 6.1) with a carrying capacity that is directly proportional to current plant quality and reproductive rate β. What is the function g?

(c) With a suitable definition of constants in this problem your equations should have the following nullclines:

$$\begin{aligned} x \text{ nullclines:} \quad & x = 0, \\ & x = 1, \\ & x = \alpha(y - 1), \\ y \text{ nullclines:} \quad & y = 0, \\ & y = Kx. \end{aligned}$$

Draw these curves in the xy plane. (There is more than one possible configuration, depending on the parameter values.)

(d) Now find the direction of motion along all nullclines in part (c). Show that under a particular configuration there is a set in the xy plane that "traps" trajectories.

(e) Define $\gamma = \alpha/(\alpha K - 1)$. Interpret the meaning of this parameter. Show that $(\gamma, K\gamma)$ is a steady state of your equations and locate it on your phase plot. Find the other steady state.

(f) Using stability analysis, show that for $\gamma > 1$, $(\gamma, K\gamma)$ is a saddle point whereas for $\gamma < 1$ it is a focus.

(g) Now show that as β decreases from large to small values, the steady state $(\gamma < 1)$ undergoes the transition from a stable to an unstable focus.

(h) Use your results in the preceding parts to comment on the existence of periodic solutions. What would be the biological interpretation of your answer?

22. Lotka's chemical model given in Section 8.8 is dynamically equivalent to the Lotka-Volterra predator-prey model. Thus modifications in the chemical kinetics should result in system(s) that exhibit limit-cycle oscillations. Explore whether the Kolmogorov conditions (see box in Section 8.8) apply to a chemical system; if so, interpret the inequalities (points 1 through 8 in the box) in the context of chemical (rather than animal) species.

23. *Exact equations and Lotka's model.* Let M and N be the functions defined by equations (60), and let V be some function satisfying

$$\frac{\partial V}{\partial x_1} = M, \qquad \frac{\partial V}{\partial x_2} = N.$$

Define

$$V_1 = \int M\, dx_1 + h(x_2),$$

$$V_2 = \int N\, dx_2 + g(x_1).$$

The integrals are to be performed with respect to one of the variables only, the other one being held fixed. Show that

$$V_1 = x_1 - \frac{k}{k_2} \ln x_1 + h(x_2),$$

$$V_2 = x_2 - \frac{k_1 A}{k_2} \ln x_2 + g(x_1).$$

If $V_1 = V_2 = V$, show that V must be given by equation (55).

24. The following equations were developed by Goodwin (1963) as a model of protein-*m*RNA interactions:

$$\frac{dM}{dt} = \frac{1}{1+E} - \alpha, \qquad \frac{dE}{dt} = M - \beta.$$

Show that this system is conservative and has oscillatory solutions.

In the remaining problems we consider systems in which it is possible to explicitly solve for limit cycles and deduce their stability by transforming variables to polar form.

25. Consider a system of equations such as (1a,b). Transform variables by defining

$$x = r \cos \theta, \qquad y = r \sin \theta.$$

(a) Show that

$$r^2 = x^2 + y^2, \qquad \theta = \arctan \frac{y}{x}.$$

(b) Show that

$$\frac{1}{2} \frac{d(r^2)}{dt} = x \frac{dx}{dt} + y \frac{dy}{dt}.$$

(c) Verify that

$$r^2 \frac{d\theta}{dt} = x \frac{dy}{dt} - y \frac{dx}{dt}.$$

26. Consider the equations

$$\frac{dx}{dt} = y, \qquad \frac{dy}{dt} = -x.$$

(b) By transforming variables, obtain

$$\frac{dr^2}{dt} = 0, \qquad \frac{d\theta}{dt} = -1.$$

(b) Conclude that there are circular solutions. What is the direction of rotation? Are these cycles stable?

27. Show that the system

$$\frac{dx}{dt} = -2y, \qquad \frac{dy}{dt} = x - 5,$$

has closed elliptical orbits. (*Hint:* Consider first transforming x to $x - 5$ and y to $y/2$ and then using a polar transformation.)

28. Consider the nonlinear system of equations

$$\frac{dx}{dt} = -y + x(x^2 + y^2 - 1) = f(x, y),$$

$$\frac{dy}{dt} = x + y(x^2 + y^2 - 1) = g(x, y).$$

Show that $r = 1$ is an unstable limit cycle of the equations.

29. Lefschetz (1977) discusses the following system of equations

$$\frac{dx}{dt} = -y + xf(x^2 + y^2),$$

$$\frac{dy}{dt} = x + yf(x^2 + y^2).$$

Show that this system is equivalent to the polar equation

$$\frac{dr}{d\theta} = rf(r^2).$$

30. Find the polar form of the following equations and determine whether periodic trajectories exist. If so, find their stability.

(a) $$\frac{dx}{dt} = \frac{2\pi y}{1 + (x^2 + y^2)^{1/2}}, \qquad \frac{dy}{dt} = \frac{2\pi x}{1 + (x^2 + y^2)^{1/2}}.$$

(b) $$\frac{dx}{dt} = y + \frac{x}{(x^2 + y^2)^{1/2}}[1 - (x^2 + y^2)],$$

$$\frac{dy}{dt} = -x + \frac{y}{(x^2 + y^2)^{1/2}}[1 - (x^2 + y^2)].$$

Problems 31 and 32 follow Appendix 1 for Chapter 8.

REFERENCES

General Mathematical Sources

Arnold, V. I. (1981). *Ordinary Differential Equations*. MIT Press, Cambridge, Mass.

Cronin, J. (1977). Some Mathematics of Biological Oscillations, *SIAM Rev., 19,* 100–138.

Golubitsky, M., and Schaeffer, D. G. (1984). *Singularity and Groups in Bifurcation Theory*. (*Applied Mathematical Sciences,* vol. 51.) Springer-Verlag, New York.

Guckenheimer, J. and Holmes, P. (1983). *Nonlinear Oscillations, Dynamical Systems, and Bifurcations of Vector Fields*. Springer-Verlag, New York.

Hale, J. K. (1980). *Ordinary Differential Equations*. Krieger, Huntington, New York.

Lefschetz, S. (1977). *Differential Equations: Geometric Theory*. 2d ed. Dover, New York.

Minorsky, N. (1962). *Nonlinear Oscillations*. Van Nostrand, New York.

Odell, G. M. (1980). Appendix A3 in L. A. Segel, ed., *Mathematical Models in Molecular and Cellular Biology*. Cambridge University Press, Cambridge.

Ross, S. (1984). *Differential Equations*. 3d ed. Wiley, New York, chap. 13 and pp. 693–695.

Oscillations (Summaries and Reviews)

Berridge, M. J., and Rapp, P. E. (1979). A comparative survey of the function, mechanism and control of cellular oscillators. *J. Exp. Biol., 81,* 217–279.

Chance, B.; Pye, E. K.; Ghosh, A. K.; and Hess, B. (1973). *Biological and Biochemical Oscillators*. Academic Press, New York.

Goodwin, B. C. (1963). *Temporal Organization in Cells*. Academic Press, London.

Hoppensteadt, F. C., ed. (1979). *Nonlinear Oscillations in Biology*. (*AMS Lectures in Applied Mathematics,* vol. 17). American Mathematical Society, Providence, R.I.

Murray, J. D. (1977). *Lectures on Nonlinear Differential Equation Models in Biology*. Clarendon Press, Oxford, chap. 4.

Pavlidis, T. (1973). *Biological Oscillators: Their mathematical analysis*. Academic Press, New York.

Rapp, P. E. (1979). Bifurcation theory, control theory and metabolic regulation. In D. A. Linkens, ed., *Biological Systems, Modelling and Control*. Peregrinus, New York.

Winfree, A. T. (1980). *The Geometry of Biological Time*. Springer-Verlag, New York.

Nerves and Neuronal Excitation

Eckert, R., and Randall, D. (1978). *Animal Physiology*. W. H. Freeman, San Francisco.

Fitzhugh, R. (1960). Thresholds and plateaus in the Hodgkin-Huxley nerve equations. *J. Gen. Physiol., 43,* 867–896.

Fitzhugh, R. (1961). Impulses and physiological states in theoretical models of nerve membrane. *Biophys. J., 1,* 445–466.

Hodgkin, A. L. (1964). *The Conduction of the Nervous Impulse*. Liverpool University Press, Liverpool.

Hodgkin, A. L., and Huxley, A. F. (1952). A quantitative description of membrane current and its application to conduction and excitation in nerve. *J. Physiol., 117,* 500–544.

Kuffler, S. W.; Nicholls, J. G.; and Martin, A. R. (1984). *From Neuron to Brain*. Sinauer Associates, Sunderland, Mass.

Morris, C. and Lecar, H. (1981). Voltage oscillations in the barnacle giant muscle fiber. *Biophys. J., 35,* 193–213.

Nagumo, J., Arimoto, S., and Yoshizawa, S. (1962). An active pulse transmission line simulating nerve axon. *Proc. IRE. 50,* 2061–2070.

Models with S-shaped ("Cubic") Nullclines

Fairen, V., and Velarde, M. G. (1979). Time-periodic oscillations in a model for the respiratory process of a bacterial culture. *J. Math. Biol., 8,* 147–157.

Goldbeter, A., and Martiel, J. L. (1983). A critical discussion of plausible models for relay and oscillation of cyclic AMP in *dictyostelium* cells. In M. Cosnard, J. Demongeot,

and A. L. Breton, eds., *Rhythms in Biology and Other Fields of Application*. Springer-Verlag, New York, pp. 173–188.

Goldbeter, A., and Segel, L. A. (1977). Unified mechanism for relay and oscillations of cyclic AMP in *Dictyostelium discoideum*. *Proc. Natl. Acad. Sci. USA, 74,* 1543–1547.

Murray, J. D. (1981). A Pre-pattern formation mechanism for animal coat markings. *J. Theor. Biol., 88,* 161–199.

Segel, L. A. (1984). *Modeling dynamic phenomena in molecular and cellular biology*. Cambridge University Press, Cambridge, chap. 6.

The Hopf Bifurcation and Its Applications

See previous references and also the following:

Marsden, J. E., and McCracken, M. (1976). *The Hopf Bifurcation and Its Applications*. (*Applied Mathematical Sciences,* vol. 19.) Springer-Verlag, New York.

Pham Dinh, T.; Demongeot, J.; Baconnier, P.; and Benchetrit, G. (1983). Simulation of a biological oscillator: The respiratory system. *J. Theor. Biol., 103,* 113–132.

Rand, R. H.; Upadhyaya, S. K.; Cooke, J. R.; and Storti, D. W. (1981). Hopf bifurcation in a stomatal oscillator. *J. Math. Biol., 12,* 1–11.

The van der Pol Oscillator

See Hale (1980), Minorsky (1962), Ross (1984) and also the following:

Jones, D. S., and Sleeman, B. D. (1983). *Differential Equations and Mathematical Biology*. Allen & Unwin, London.

van der Pol, B. (1927). Forced oscillations in a circuit with nonlinear resistance (receptance with reactive triode). *Phil. Mag.* (London, Edinburgh, and Dublin), *3,* 65–80.

van der Pol, B., and van der Mark, J. (1928). The heart beat considered as a relaxation oscillation, and an electrical model of the heart. *Phil. Mag.* (7th ser.), *6,* 763–775.

Limit Cycles in Population Dynamics

Coleman, C. S. (1983). Biological cycles and the five-fold way. Chap. 18 in M. Braun, C. S. Coleman, and D. Drew, eds., *Differential Equation Models*. Springer-Verlag, New York.

Edelstein-Keshet, L. (1986). Mathematical theory for plant-herbivore systems. *J. Math. Biol., 24,* 25–58.

Freedman, H. I. (1980). *Deterministic Mathematical Models in Population Ecology*. Dekker, New York.

Kolmogorov, A. (1936). Sulla Teoria di Volterra della Lotta per l'Esistenza, *G. Ist. Ital. Attuari, 7,* 74–80.

May, R. M. (1974). *Stability and Complexity in Model Ecosystems*. 2d ed. Princeton University Press, Princeton, N.J.

Rescigno, A., and Richardson, I. W. (1967). The struggle for life I: Two species, *Bull. Math. Biophys., 29,* 377–388.

Oscillations in Chemical Systems

Belousov, B. P. (1959). An oscillating reaction and its mechanism. *Sb. Ref. Radiats. Med.*, Medgiz, Moscow. p. 145. (In Russian.)

Bray, W. C. (1921). A periodic reaction in homogeneous solution and its relation to catalysis. *J. Amer. Chem. Soc., 43,* 1262–1267.

Degn, H. (1972). Oscillating chemical reactions in homogeneous phase. *J. Chem. Ed., 49,* 302–307.

Escher, C. (1979). Models of chemical reaction systems with exactly evaluable limit cycle oscillations. *Z. Physik B, 35,* 351–361.

Ghosh, A., and Chance, B. (1964). Oscillations of glycolytic intermediates in yeast cells. *Biochem. Biophys. Res. Commun., 16,* 174–181.

Hyver, C. (1984). Local and global limit cycles in biochemical systems. *J. Theor. Biol., 107,* 203–209.

Lotka, A. J. (1920). Undamped oscillations derived from the law of mass action. *J. Amer. Chem. Soc., 42,* 1595–1599.

Nicolis, G., and Portnow, J. (1973). Chemical oscillations. *Chem. Rev., 73,* 365–384.

Pye, K., and Chance, B. (1966). Sustained sinusoidal oscillations of reduced pyridine nucleotide in a cell-free extract of *Saccharomyces carlsbergensis. Proc. Natl. Acad. Sci., 55,* 888–894.

Schnakenberg, J. (1979). Simple chemical reaction systems with limit cycle behavior, *J. Theor. Biol., 81,* 389–400.

Sel'kov, E. E. (1968). Self-oscillations in glycolysis. A simple kinetic model. *Eur. J. Biochem., 4,* 79–86.

Tyson, J. J. (1979). Oscillations, bistability, and echo waves in models of the Belousov-Zhabotinskii reaction. In O. Gurel and O. E. Rossler, eds., *Bifurcation Theory and Applications in Scientific Disciplines. Ann. N.Y. Acad. Sci., 316,* pp. 279–295.

Zhabotinskii, A. M. (1964). Periodic process of the oxidation of malonic acid in solution. *Biofizika, 9,* 306–311. (In Russian.)

Circadian and Physiological Oscillations

See Winfree (1980) as well as the following:

Brown, F. A.; Hastings, J. W.; and Palmer, J. D. (1970). *The Biological Clock: Two Views.* Academic Press, New York.

Bunning, E. (1967). *The Physiological Clock.* 2d ed. Springer-Verlag, New York.

Edmunds, L. N., ed. (1984). *Cell Cycle Clocks.* Marcel Dekker, New York.

Kronauer, R. E.; Czeisler, C. A.; Pilato, S. F.; and Moore-Ede, M. C. and Weitzman, E. D. (1982). Mathematical model of the human circadian system with two interacting oscillators. *Am. J. Physiol., 242,* R3–R17.

Moore-Ede, M. C.; Czeisler, C. A., eds. (1984). *Mathematical Models of the Circadian Sleep-Wake Cycle.* Raven Press, New York.

Moore-Ede, M. C.; Sulzman, F. M.; and Fuller, C. A. (1982). *The Clocks that Time Us.* Harvard University Press, Cambridge, Mass.

Reinberg, A., and Smolensky, M. H. (1984). *Biological Rhythms and Medicine.* Springer-Verlag, New York.

Strogatz, S. (1986). *The Mathematical Structure of the Human Sleep-Wake Cycle, Lecture Notes in Biomathematics, 69,* Springer-Verlag, New York.

Ward, R. R. (1971). *The Living Clocks.* Knopf, New York.

APPENDIX 1 TO CHAPTER 8: SOME BASIC TOPOLOGICAL NOTIONS

Many of the theorems that apply to systems of two ordinary differential equations such as (1a,b) are based on what are called *topological properties* of curves in the plane. While the topological theory itself is abstract and exceptionally beautiful, we shall avoid formal details, giving instead a descriptive outline of some key concepts. (See Arnold, 1981, for an introductory summary.)

Imagine a vector field in the xy plane. The vector field may have been generated by the set of equations (1a,b). Figure 8.24 serves as an example. In this vector field we place a *simple oriented closed curve;* (we may think of this curve as a deformed circle along which some point moves in a particular direction). We first consider arbitrary curves as "test" objects that are used to understand the vector field. (Only later will we turn to closed curves generated by the vector field itself.) Tracing the path of a single point around the test curve we may follow the rotation of a field vector attached to the point. If the curve does not go through any singular point [point at which $F = G = 0$ in equations (1)], the rotation will be continuous as the curve is traversed, and the field vector will have returned to its original orientation when the point has returned to its initial position. The *number of revolutions* and the *direction of rotation* executed by the field vector depend on details of the flow patterns. (Several possibilities are shown in Figure 8.24.) The *index of a curve* is the number of revolutions, and the sign of the index reflects whether the rotation is in the same sense or in an opposite sense to that of the curve.

A number of properties make the concept of the index important:

1. The index does not change if the curve is distorted, twisted, or enlarged, provided that in the process of change the curve does not go through any singular points.
2. Similarly, if the vector field is warped, distorted, or rearranged, the index of the curve will not change if no singular points cross the curve or are on the curve during the process.

Using such properties it can be shown (see Problem 31a) that the following fact holds true:

3. The index of a simple closed curve is zero unless there is at least one singular point in the region bounded by the curve.

We now define the *index of a singular point P* as the index of any circle of *small* radius centered at P. (See Figure 8.24.) According to property 1 the radius of this circle is immaterial as long as the curve encloses only *one* singular point and does not itself go through any singular points.

4. The indices of common isolated singular points are as follows [see Figure 8.24(f–h)]:
   - **(i)** The index of a node is $+1$.
   - **(ii)** The index of a focus is $+1$.
   - **(iii)** The index of a center is $+1$.
   - **(iv)** The index of a saddle point is -1.

(These are independent of stability in cases 1 and 2 and independent of direction of rotation in cases 3 and 4. See problem 31b.)

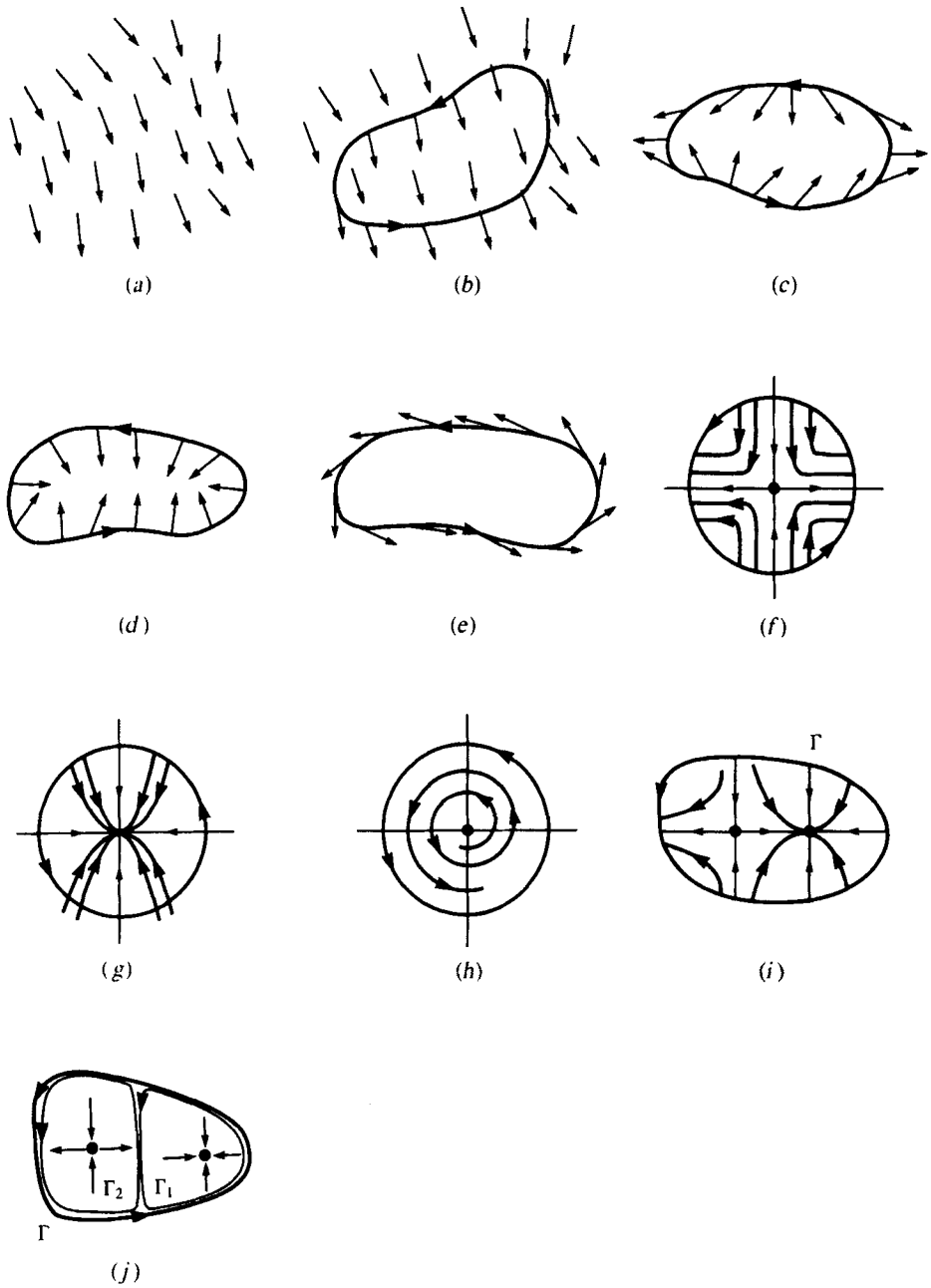

Figure 8.24 *(a) A vector field. (b) A test curve Γ; the vector field does not complete a revolution as curve is traversed (index = 0). (c) The field vector rotates by one revolution in the direction opposite to the curve (index = −1). (d) The field vector rotates by one revolution in the same direction (index = +1). (e) Limit cycle or any closed periodic trajectory (index = +1). (f) Saddle point (index = −1). (g) Node (index = +1). (h) Focus/center (index = +1). (The index of a singular point = index of a small circle encircling the point.) (i) The index of a test curve encircling several points equals (j) the sum of indices of the individual points. [After Arnold (1981).]*

Now consider a curve Γ that surrounds a region containing several singular points. Then the following can be proved:

5. The index of a curve is equal to *the sum of the indices of singular points* in the region D which it surrounds.

This result can be established by considering a picture similar to Figure 8.24(i, j). Here two artificial extensions of the original curve have been so added that their net contribution to the total rotation "cancels." The index of Γ must therefore be the same as that of Γ_1 plus Γ_2. However, according to property 1, these can be distorted to small circles about their respective singular points without change of index. This verifies the claim. (The argument is made more formal by giving a rigorous definition of index in terms of a *line integral* and demonstrating that the sum of line integrals around Γ_1 and Γ_2 equals the line integral of Γ. Students who have had advanced calculus may recognize Figure 8.24(i, j) as a familiar trick used in Green's theorem.)

These notions are useful in establishing the relation between a periodic solution of equations (1a,b) and singular points (or in our popular phrasing, steady states) of the flow $(F(x, y), G(x, y))$. According to previous remarks, a periodic solution corresponds to a solution curve that is itself simple and closed; the flow causes the point $(x(t), y(t))$ to rotate around this curve. In particular, the field vectors are tangent to the curve itself. By referring to Figure 8.24(e) we can clearly see that the field vector must therefore execute *one complete rotation* in the positive sense as the curve is traversed. We have thus observed the following:

6. The index of a closed (periodic-orbit) solution curve is $+1$.

Collecting all of our remarks and observations, we conclude the following:

7. **(a)** A limit cycle (or any closed periodic orbit) must contain at least one singular point.
(b) If it contains *exactly* one, that singular point must be a node, a focus, or a center.
(c) If it contains *more than* one, the number of saddle points must be one less than the total number of foci, nodes, and centers. (Note that only these four types of singular points are permitted).

More discussion of these observations is given in the problems. We now consider their applicability. First, an important comment is that the properties we have described derive from the basic topology of the plane. It is possible to generalize ideas to other "locally flat" objects called *manifolds* (such as the surface of a sphere, a torus, and so forth.) We shall leave the abstract development at this point and remark merely that conclusions of this section are specific to two-dimensional systems. In three dimensions, for example, more complicated flow patterns may accompany closed periodic trajectories, so that the number and locations of singular points may have no bearing on the presence of a limit cycle.

While the index properties do not predict whether limit cycles occur, they do shed light on restrictions that apply. Using these we can rule out, for example, any closed periodic trajectories about regions that contain exactly two nodes or exactly one node and one saddle point.

PROBLEMS FOR APPENDIX 1*

31. *Index of a curve*

(a) Give reasons to support the assertion that the index of a simple closed curve is zero unless there is at least one singular point in the region bounded by the curve.

(b) Show that the index of a singular point is independent of its stability.

(c) A rigorous definition of the index of a curve is as follows:
for the vector field $\mathbf{V} = (F(x, y), G(x, y))$ the quantity

$$\frac{G(x, y)}{F(x, y)}$$

is the slope of a field vector in the xy plane. Define

$$d\phi = d\left(\arctan \frac{G}{F}\right).$$

Show that

$$d\phi = \frac{GdF - FdG}{F^2 + G^2} \qquad (G \neq 0).$$

The rest of this problem requires familiarity with line integrals.

***(d)** Now define the index of a closed curve ind γ by the following line integral

$$\text{ind } \gamma = \frac{1}{2\pi} \int_\gamma d\phi.$$

Show that this definition corresponds to the concept of index previously described.

***(e)** Use this definition together with Green's theorem to verify the claim that the index of a curve is equal to the sum of the indices of all singular points inside the region bounded by the curve. [*Hint:* Consult figure (*a*) for problem 32.]

32. **(a)** Show or give reason for the assertion that the index of a node, a focus, or a center is $+1$ and that of a saddle point is -1.

(b) Which of the cases shown in the accompanying figures is possible?

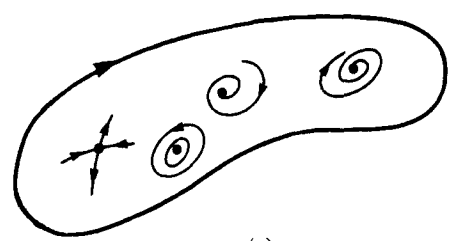

(*a*)

* Problems preceded by asterisks (*) are especially challenging.

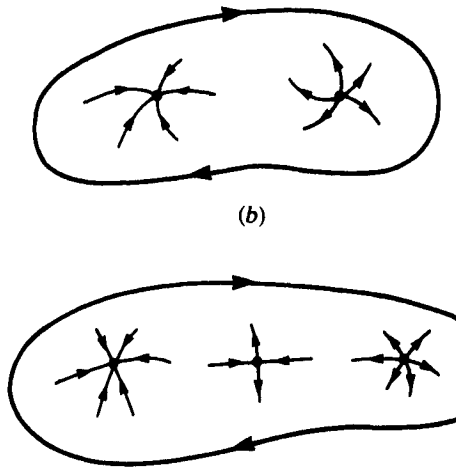

Figure for problem 32.

APPENDIX 2 TO CHAPTER 8: MORE ABOUT THE POINCARÉ-BENDIXSON THEORY

In this appendix we collect some mathematical terminology commonly encountered in the Poincaré-Bendixson theory. Using these definitions we then give a more precise statement of the Poincaré-Bendixson theorem. Also included is a proof of Bendixson's negative criterion.

Definitions

1. An orbit Γ through the point P is the curve
$$\{\mathbf{x}_P(t) \,|\, -\infty < t < \infty \text{ with } \mathbf{x}_P(0) = P\}.$$
2. A positive semiorbit Γ^+ through P is the curve
$$\{\mathbf{x}_P(t) \,|\, 0 \leq t < \infty \text{ with } \mathbf{x}_P(0) = P\}.$$
Similarly the negative semiorbit Γ^- is defined for $-\infty < t \leq 0$.
3. The ω limit set of Γ is the set of points in R^2 that are approached along Γ with increasing time. Similarly, the α limit set of Γ is defined as the set of points approached with decreasing time.
4. A *limit cycle* is a periodic orbit Γ_0 that is the ω limit set or the α limit set for all other orbits in some neighborhood of Γ_0.

To paraphrase, we draw a distinction between solutions of equations (1a,b) for all time (which are represented by orbits Γ in the plane) and those for $t \geq t_0$ or $t \leq t_0$ (represented by semiorbits Γ^+ and Γ^-). We have also introduced above the important notion of *limiting sets;* these come in two varieties (ω and α) depending on whether the limit is taken for $t \to \infty$ or $t \to -\infty$ respectively. They are thus the point sets that are approached along a trajectory in the forward (ω) or reverse (α) time direction.

A limit cycle is a special periodic solution of the autonomous dynamic system (1a,b) that is also simultaneously a limiting set for nearby trajectories. Physically this means that for $t \to \infty$ (or $t \to -\infty$, depending on stability) a solution that starts out close to the periodic solution will eventually be indistinguishable from it. (Of course, from the mathematical standpoint the two will never be exactly equal during finite time.)

We now state the Poincaré-Bendixson theorem, whose proof is to be found in numerous advanced books on ODEs (for example, see Hale, 1980):

> ***Theorem 1: The Poincaré-Bendixson Theorem:***
>
> A bounded semiorbit that does not approach any singular point is either a closed periodic orbit or approaches a closed periodic orbit.

Finally, we prove Bendixson's criterion (stated in Section 8.3) using Green's theorem.

A Proof of Bendixson's Criterion

Suppose C is a closed-curve trajectory in the simply connected region D. Then by Green's theorem

$$\int_C F(x, y)\, dy - G(x, y)\, dx = \int\int_S \left(\frac{\partial F}{\partial x} + \frac{\partial G}{\partial y}\right) dx\, dy, \tag{77}$$

where S is the region contained within the curve C.

For the system of equations (1a,b) we have the following relations:

$$\frac{dx}{dy} = \frac{dx/dt}{dy/dt} = \frac{F(x, y)}{G(x, y)}, \tag{78}$$

so that $G(x, y)\, dx = F(x, y)\, dy$.

The integral of the LHS above must therefore be zero, forcing the conclusion that

$$\int\int_S \left(\frac{\partial F}{\partial x} + \frac{\partial G}{\partial y}\right) dx\, dy = 0. \tag{79}$$

The quantity $\partial F/\partial x + \partial G/\partial y$ will not have a vanishing integral over S unless it is (1) always zero or (2) alternately positive *and* negative in S. This proves the theorem.